Project Title

MECHANISM OF THERMAL RUNAWAY IN VRLA BATTERIES AND METHODS TO SUPPRESS IT

FINAL TECHNICAL REPORT

BY

PROF. DETCHKO PAVLOV (PRINCIPAL INVESTIGATOR)
FULL MEMBER OF THE BULGARIAN ACADEMY OF SCIENCES

(DECEMBER 2004)

UNITED STATES ARMY

EUROPEAN RESEARCH OFFICE OF THE U.S. ARMY

LONDON, ENGLAND

CONTRACT NUMBER: N62558-03-M-0805

CONTRACTOR: CENTRAL LABORATORY OF ELECTROCHEMICAL POWER SOURCES (CLEPS), LEAD-ACID BATTERIES DEPARTMENT

Report Documentation Page

Form Approved
OMB No. 0704-0188

1. REPORT DATE	2. REPORT TYPE	3. DATES COVERED
2004	**N/A**	**-**

4. TITLE AND SUBTITLE	5a. CONTRACT NUMBER
Mechanism Of Thermal Runaway In Vrla Batteries And Methods To Suppress It	5b. GRANT NUMBER
	5c. PROGRAM ELEMENT NUMBER
6. AUTHOR(S)	5d. PROJECT NUMBER
	5e. TASK NUMBER
	5f. WORK UNIT NUMBER
7. PERFORMING ORGANIZATION NAME(S) AND ADDRESS(ES) **Bulgarian Academy Of Sciences**	8. PERFORMING ORGANIZATION REPORT NUMBER
9. SPONSORING/MONITORING AGENCY NAME(S) AND ADDRESS(ES)	10. SPONSOR/MONITOR'S ACRONYM(S)
	11. SPONSOR/MONITOR'S REPORT NUMBER(S)

12. DISTRIBUTION/AVAILABILITY STATEMENT
Approved for public release, distribution unlimited

13. SUPPLEMENTARY NOTES
The original document contains color images.

14. ABSTRACT
The technical objective of the current project is to disclose the mechanism of the processes leading to Thermal Runaway (TRA) in VRLA batteries during overcharge. The TRA effect is related to an uncontrolled temperature rise reaching very high values of 80-100oC on battery overcharge. An appropriate experimental set up was built for the purposes of the project work. It allowed us to monitor 5 cell parameters: current, positive and negative plate potentials, temperature and gassing rate of the cells. The experiments show that TRA may occur when the cell is exposed on continuous overcharge at a voltage higher than a certain critical value. It has been established that the reactions that proceed at the two types of electrodes are in selfaccelerating interrelation. At the positive plates, a reaction of water decomposition and evolution of oxygen proceeds. O2 is reduced at the negative plates whereby heat is released. Consequently, the temperature in the cell rises. The elevated temperature accelerates the reaction of water decomposition and oxygen evolution at the positive plates. Thus, the processes at the two types of plates accelerate each other. However, with increase of temperature, the heat exchange between the cell and the surrounding medium increases. When the exchanged heat becomes equalt to the heat generated in the cell by the reactions at the negative plates, the cell temperature reaches a maximum. This phenomenon was called self-accelerating interrelation between the reactions of the oxygen cycle (SAIR), it refers to the spontaneous current increase. The thermal runaway (TRA), reflecting the temperature rise, and the SAIR are two sides of one and the same phenomenon designated by SAIR-TRA. Up to now the processes involved in the above phenomenon have been known as TRA effect. The increase in cell temperature and current during TRA depends strongly on the type of the separator used, the cell voltage, and the history of battery operation. As a result of the TRA phenomena the cell structure changes, which suppresses further temperature rise. The results of the above investigations imply that it is possible to suppress the TRA phenomena and eliminate the thermal problems during VRLAB operation through selection of appropriate type of separator and appropriate mode of battery operation.

15. SUBJECT TERMS					
16. SECURITY CLASSIFICATION OF:			17. LIMITATION OF ABSTRACT	18. NUMBER OF PAGES	19a. NAME OF RESPONSIBLE PERSON
a. REPORT **unclassified**	b. ABSTRACT **unclassified**	c. THIS PAGE **unclassified**	**SAR**	**38**	

Standard Form 298 (Rev. 8-98)
Prescribed by ANSI Std Z39-18

TABLE OF CONTENTS

	Page
ABSTRACT	**3**
INTRODUCTION	**4**
EXPERIMENTAL SET-UP	**5**
1. Experimental cells	**5**
2. Equipment used	**6**
3. Model cells	**6**
4. Research approach	**7**
EXPERIMENTAL RESULTS AND DISCUSSION	**8**
1. Thermal phenomena in cells with AGM separators	**8**
2. Thermal phenomena in MAGM cells	**18**
3. Temperature dependence of cell voltage and of positive and negative plate potentials	**22**
4. Analyses of the active materials after the polarization tests	**25**
5. Chemical and electrochemical reactions involved in the oxygen cycle and proceeding at the two types of electrodes	**30**
CONCLUSIONS	**34**
What should be done within a next stage of investigations of the SAIR-TRA phenomenon?	**36**
LITERATURE CITED	**37**

ABSTRACT

The technical objective of the current project is to disclose the mechanism of the processes leading to Thermal Runaway (TRA) in VRLA batteries during overcharge. The TRA effect is related to an uncontrolled temperature rise reaching very high values of 80-100^{o}C on battery overcharge. An appropriate experimental set up was built for the purposes of the project work. It allowed us to monitor 5 cell parameters: current, positive and negative plate potentials, temperature and gassing rate of the cells. The experiments show that TRA may occur when the cell is exposed on continuous overcharge at a voltage higher than a certain critical value. It has been established that the reactions that proceed at the two types of electrodes are in self-accelerating interrelation. At the positive plates, a reaction of water decomposition and evolution of oxygen proceeds. O_2 is reduced at the negative plates whereby heat is released. Consequently, the temperature in the cell rises. The elevated temperature accelerates the reaction of water decomposition and oxygen evolution at the positive plates. Thus, the processes at the two types of plates accelerate each other. However, with increase of temperature, the heat exchange between the cell and the surrounding medium increases. When the exchanged heat becomes equalt to the heat generated in the cell by the reactions at the negative plates, the cell temperature reaches a maximum. This phenomenon was called "*self-accelerating interrelation between the reactions of the oxygen cycle (SAIR)*", it refers to the spontaneous current increase. The thermal runaway (TRA), reflecting the temperature rise, and the SAIR are two sides of one and the same phenomenon designated by SAIR-TRA. Up to now the processes involved in the above phenomenon have been known as TRA effect.

The increase in cell temperature and current during TRA depends strongly on the type of the separator used, the cell voltage, and the history of battery operation. As a result of the TRA phenomena the cell structure changes, which suppresses further temperature rise.

The results of the above investigations imply that it is possible to suppress the TRA phenomena and eliminate the thermal problems during VRLAB operation through selection of appropriate type of separator and appropriate mode of battery operation.

Keywords: lead-acid battery, thermal runaway, oxygem cycle, valve-regulated lead-acid battery, thermal effects in lead-acid batteries

INTRODUCTION

VRLA batteries comprise two electrochemical systems: (a) the $Pb/PbSO_4$ and $PbO_2/PbSO_4$ system that accumulates and generates energy, and (b) the H_2O/O_2 and O_2/H_2O oxygen cycle, which operates during battery overcharge. As all electrochemical processes involved in the oxygen cycle are temperature dependent, the phenomenon known as "thermal runaway" (TRA) occurs. As discussed in our 2nd and 3rd Interim Reports, the TRA effect occurs on polarization at constant voltage. Under such conditions, the current increases with time of constant voltage polarization, which leads to temperature rise in the cell and hence accelerates the electrochemical processes. These processes are influenced by the type and properties of the separator used. That is why we performed investigations with two types of separators: absorptive glass mat (AGM) and AGM modified with polymeric emulsion (MAGM). The present Final Report compares the evolution of TRA phenomena in cells with AGM and MAGM separators.

All experiments were performed with fully charged cells in which only the reactions of the oxygen cycle proceed. As the TRA effect occurs on constant voltage polarization of the cells, we conducted investigations at different, but constant, voltages. The changes in 6 cell parameters were followed with time of polarization. These changes were induced by both the heat effects of the reactions and the Joule heat. The dependence of cell temperature on current density was selected as the generalized function. On completion of the above series of thermal investigations of the cells, a series of polarization tests was performed to determine the temperature coefficients of the reactions involved in the oxygen cycle at the positive and at the negative plates.

In an attempt to establish the influence of the TRA effect on the active masses we performed various analyses aimed to determine the phase composition and structure of the positive and negative active masses as well as their crystal morphology. The obtained results of these analyses for the cells with different separators will be compared in this report.

EXPERIMENTAL SET-UP [1]

1. Experimental cells

Figure 1 presents a diagram of the parameters that change during cell overcharge when the cell voltage is increased from U_1 to U_2. The latter change causes the potentials of the positive (φ+) and of the negative (φ-) plates (electrodes) to change, as a result of which the current i_1 that flows through the cell increases to i_2. When the cell is fully charged, the only reaction that proceeds at the positive plates is the reaction of oxygen evolution (i_{O2}^+ is the rate of this reaction). At the negative plates, part of the evolved oxygen (i_{OC}) is reduced and hydrogen is evolved (i_{H2}). The oxygen that is reduced at the negative plates forms a closed oxygen cycle (OxCy). Another part of the evolved oxygen ($i_{O2\ out}$) leaves the cell. The ratio i_{OC}/i_{O2}^+ gives the efficiency of the closed oxygen cycle (η_{OC}). The reduction of oxygen at the negative plates is an exothermic reaction, i.e. heat is released, which causes the temperature in the cell to rise from t^o_1 to t^o_2.

On prolonged polarization of the cell, at a pre-set cell voltage, a self-accelerated temperature rise occurs. The cell temperature increases and, if the current is not very high and the heat exchange between the cell and the surrounding medium is good, the temperature the may reach up to 80^{o}C. Let us call this phenomenon thermal rise (TR). However, in the opposite case the temperature rise may continue further to reach values higher than 100^{o}C as a result of which the acid in the cell boils, the cell case softens and swells, which may cause the electrical circuit in the battery to break. This phenomenon is called thermal runaway (TRA).

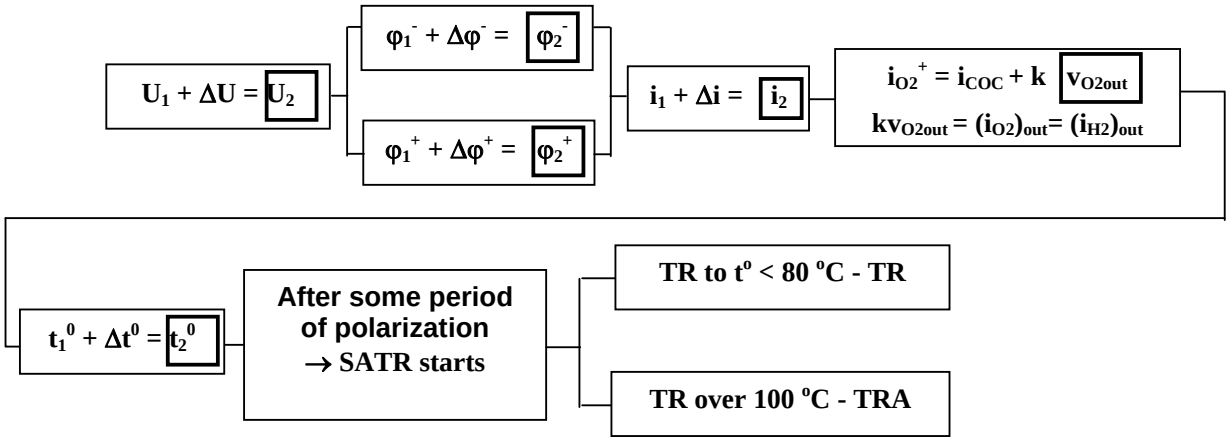

Fig. 1. Parameters that change during cell charge with increase of the cell voltage

In an attempt to identify the phenomena that proceed on thermal rise and thermal runaway we measured the following cell parameters (marked with bold squares in Fig.1) and monitored how they change with the time of polarization:

U – cell voltage

φ^+ - positive plate potential *vs.* Ag/Ag_2SO_4 reference electrode

φ^- - negative plate potential *vs.* Ag/Ag_2SO_4 reference electrode

i – current flowing through the cell

t^o – cell temperature

dV_{out}/dt - rate of gas leaving the cell

$V_{out} = V_{O2\ out} + V_{H2\ out}$ – total volume of gas released from the cell for the time of polarization

2. Equipment used [2]

- Bitrode SCN 10-5 test modules were used to maintain constant current or constant voltage in the model cells.
- The potentials of the positive and of the negative plates were measured versus a specially designed and constructed Ag/Ag_2SO_4 reference electrode.
- A 16-channel computerized data acquisition system was specially designed and constructed to collect the data from the measuring instruments.
- The changes in cell temperature were monitored through thermocouples mounted in the cells and the obtained data were continuously collected and saved in a computer.
- When the cell valves opened, the rate of the released gas was measured with the help of a computerized gassing rate monitoring (GRM) system (own design).

3. Model cells

Model cells 2V/4Ah were assembled using specially designed and produced transparent polymer cases, positive and negative plates with grids cast from PbSn alloy. The plates were formed and dried (the negative ones in nitrogen atmosphere), then they were weighed and mounted dry charged in the cells. AGM separators (Hollingsworht & Vose) and modified AGM (MAGM) separators developed in our laboratory were used. The separators were inserted between the plates under

compression so that their thickness was reduced by 7 or 22%. Each cell was outfitted with a valve, a Ag/Ag_2SO_4 reference electrode and a thermocouple. The gas leaving the cell through the valve was forced to pass through a flow meter (the GRM system).

4. Research approach

Two series of experimental cells were manufactured: one with AGM and the other one with MAGM separators. Two series of experiments (tests) were performed as follows:

(a) The first series of experiments (tests) was aimed to investigate the cycle life performance of AGM and MAGM cells as well as the influence of cell polarization at constant voltage and constant current. The results of these investigations were discussed in detail in our 2nd Interim Report [2].

(b) The second series of experiments (tests) with AGM and MAGM cells was aimed to investigate the mechanism of the thermal runaway phenomenon itself. A detailed description of the behaviour of the MAGM cells under test was presented in our 3rd Interim Report [3]. In the present Final Report we will disclose the mechanism of the TRA effect on grounds of the test results for two experimental cells, one with AGM and the other one with MAGM separators. The test results for the remaining 4 AGM cells and 7 MAGM cells are analogous, so they will not be discussed in this report. The behaviour of these cells is indicative not only of the processes that occur on thermal runaway, but also of the influence of the separator on these processes.

EXPERIMENTAL RESULTS AND DISCUSSION

1. Thermal phenomena in cells with AGM separators

Figure 2 shows the changes in the five measured parameters on polarization of the AGM cell at constant voltage of 2.50 V (Fig. 2A), 2.45 V (Fig. 2B) and 2.40 V (Fig. 2C), respectively.

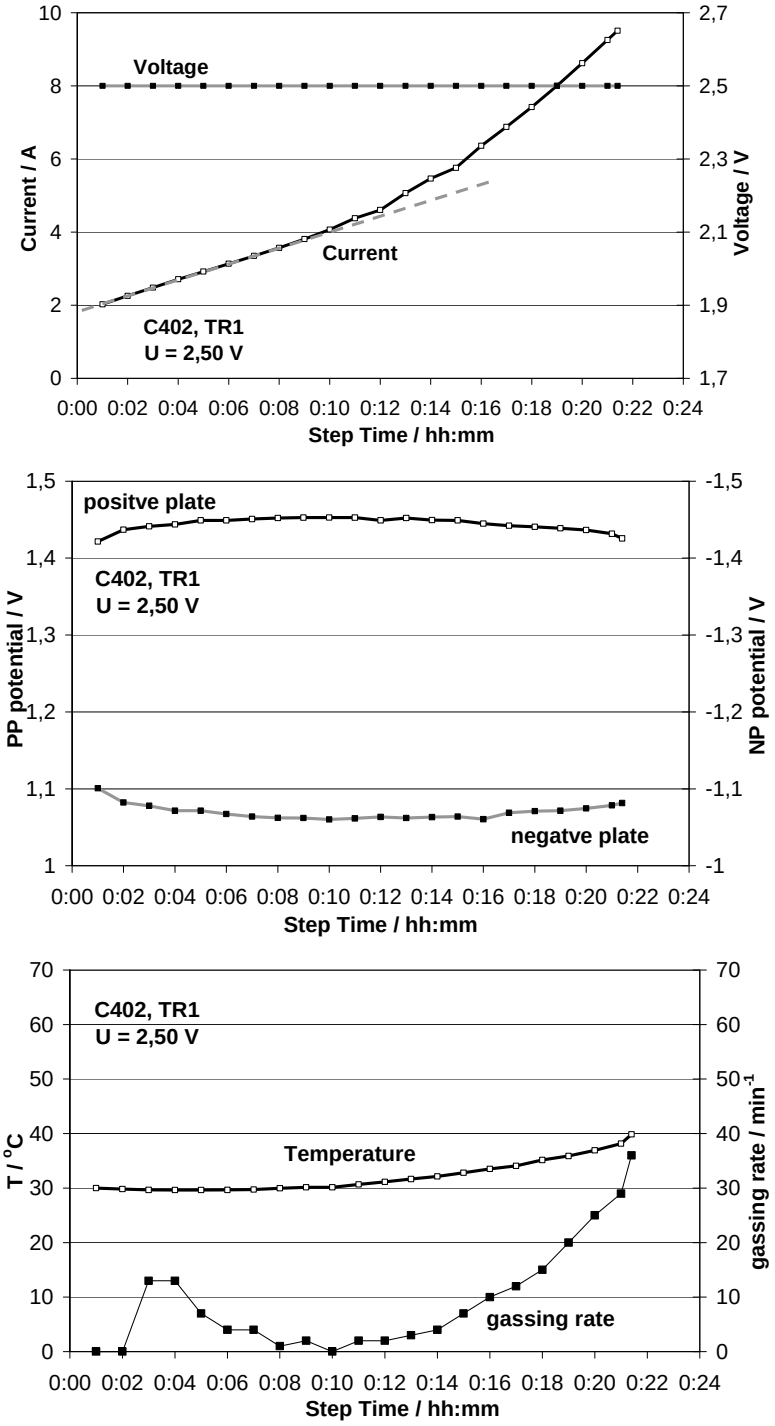

Fig. 2a. Changes in U, I, φ^+, φ^-, T^o and gassing rate during polarization of the cell at different constant voltages: 2.50 V (Fig. 2a); 2.45 V (Fig. 2b) and 2.40 (Fig. 2c).

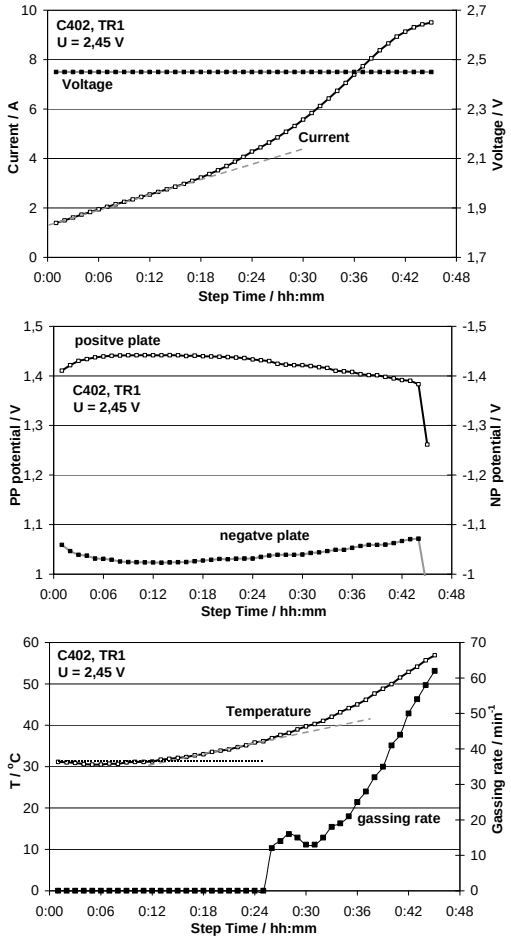

Fig. 2b.

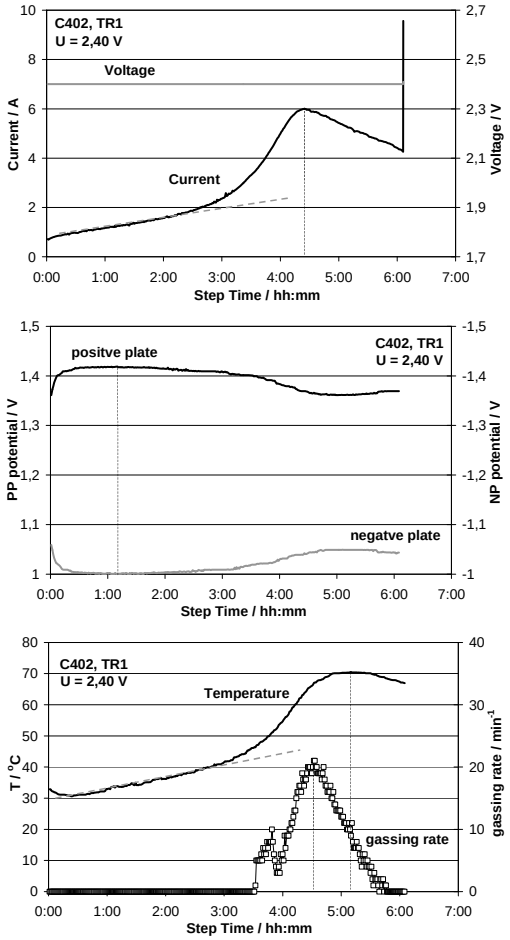

Fig. 2c.

The following conclusions can be drawn on grounds of the above experimental results:

(a) During polarization of the cell at 2.50 V, the current reaches a value of 9 A within 22 min. The same current value is reached after 43 min when the polarization is conducted at 2.45 V, and after 4.5 h when the cell is polarized at 2.40 V. The current vs. polarization time curve features a maximum (I_{max}). The cell temperature exhibits analogous behaviour.

(b) Both the current and the temperature curves feature a linear section at the beginning of polarization within which the increase of *i* or *T* is proportional to the time of polarization. After that period of linear increase, some processes occur in the cell that cause both the current and the temperature to increase at a higher rate.

(c) On cell polarization at 2.40 V (Fig. 2C), several maximums appear in the curves: first the φ^+ peak in the φ^+/t curve occurs with the corresponding φ^- minimum in the φ^-/t curve, followed by the i_{max} in the current transient and the maximum in the gassing rate/time curve, and finally the T_{max} in the temperature curve. This behaviour of the measured parameters indicates that on polarization of the cell at constant voltage (U), the processes involved in the oxygen cycle (OxCy) pass through different stages to reach a certain steady state.

Figure 3 presents the current and temperature dependencies as a function of the quantity of electricity flowing through the cell on polarization at 2.40 V. The characteristic points marking the onset of distinct changes in the profiles of the two curves are highlighted in the figure. Four regions can be distinguished clearly.

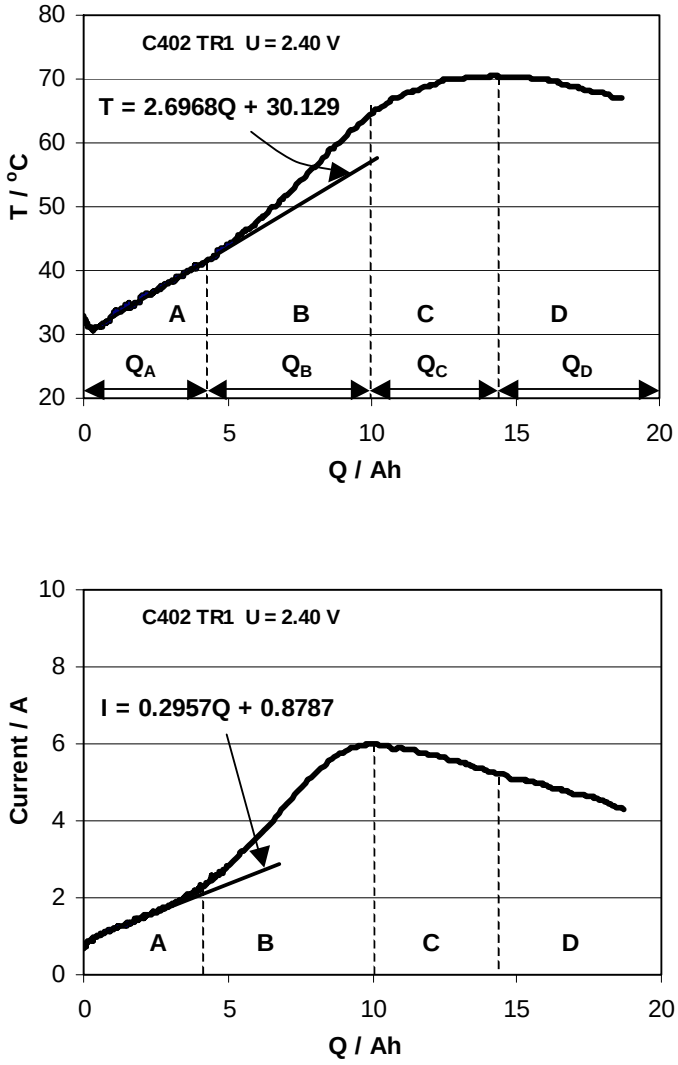

Fig. 3. Dependence of the cell temperature and overcharge current on the electricity accumulated by the cell at U = 2.40 V.

Region A (Fig. 3). Electric current flows through the cell generating Joule heat and some exothermal chemical reactions proceed which also generate heat. These heat effects cause the cell temperature to rise following a linear dependence on the quantity of electricity flowing through the cell, Q.

$$T = 2.70\ Q + 20.12 \qquad (A)$$

The elevated temperate accelerates the electrochemical and chemical reactions as a result of which the current increases also following a linear dependence on the quantity of electricity:

$$i = 0.30\ Q + 0.88 \qquad (B)$$

The above linear profile of the temperature increase continues until a quantity of electricity Q_A is introduced into the cell.

Region B (Fig. 3). When a Q_A quantity of electricity flows through the cell, some processes start which lead to an increase in current *i* greater than the one predicted by the linear equation. This current increase continues until the maximum value I_{max} is reached. During this time a quantity of electricity Q_B flows through the cell. Faster current increase is possible only if the accelerated electrochemical reactions on one of the electrodes causes the reactions on the other electrode to proceed at a higher rate, too, i.e. when the reactions at the two electrodes are interrelated. The reactions that proceed at the negative electrode (oxygen reduction) are associated with heat release. The latter causes the cell temperature to increase, which in turn accelerates the reactions at the positive electrode (water decomposition and oxygen evolution). The evolution of more oxygen at the positive plate results in a more intense oxygen flow towards the negative plate. Hence, the rate of oxygen reduction at the negative plate will increase and so will the amount of released heat, too. The latter will cause further temperature rise. Thus, the processes proceeding at the two types of electrodes get into a circular self-accelerating interrelation. This self-accelerating influence of the processes at the two electrodes is presented schematically in Fig. 4. Let us call this phenomenon *self-accelerating interrelation between the reactions of the OxCy (SAIR)* [4]. The rapid current increase leads to a rapid temperature rise (Fig. 3b) also known as thermal runaway (TRA). SAIR and TRA are two sides of one and the same phenomenon which we can call SAIR-TRA. Up to now the above phenomenon is known as TRA, though this designation reflects only half of the processes involved in the phenomenon.

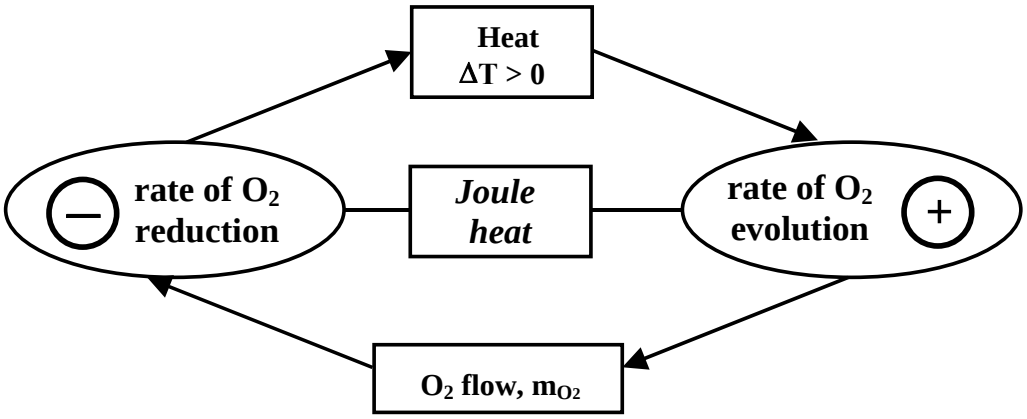

Fig. 4. Schematic representation of the self-accelerating interrelations between the reactions of the oxygen cycle in a VRLA cell.

Region C (Fig. 3). The cell temperature increases further after region B, when another 5.0 Ah flow through the cell, to reach the maximum value T_{max}. Within this region C, which takes more than an hour, the current decreases from 6 to 5 A and hence the Joule heat decreases, too. However, the cell temperature continues to rise. It follows then that the temperature increase is a result of the heat effects of the reactions involved in the oxygen cycle. After a quantity of electricity Q_C flows through the cell, the cell temperature reaches its maximum value T_{max}. The latter is determined by (depends on?) the following phenomenon. With increase of temperature in the cell, the difference between the cell temperature and the temperature of the surrounding medium increases. Hence, the heat flow that leaves the cell increases, too. When the heat leaving the cell per unit time equals the heat generated by the reactions in the cell per unit time, the cell temperature reaches its maximum value T_{max}. The fact that i_{max} and T_{max} are reached when different quantities of electricity have passed through the cell indicates unequivocally that temperature increase is due to the heat effects of some *chemical reactions* of oxygen reduction. When Q_C quantity of electricity flows through the cell, its temperature begins to decrease with further decrease of the current.

Region D (Fig. 3). Within this region, both the current and the temperature decrease reaching stationary values. During this period, too, there is an interrelation between the processes that occur at the two electrodes. The lower current flowing through the cell within the D region decreases the oxygen flow that is generated at the positive plate. On reduction of this oxygen, less heat will be generated per unit time. The heat

leaving the cell per unit time will be greater than the generated one and hence the cell temperature will decrease. Consequently, the rate of the reactions of oxygen evolution at the positive plate will be slowed down. Thus, the interrelation between the processes ocurrign at the two electrodes will have a negative effect. This phenomenon will continue until the heat generated in the cell per unit time becomes equal to the heat leaving the cell per unit time. Only then will the stationary stage of the OxCy begin.

Figure 5 presents the i/Q and T/Q curves for the different cell voltages within the A region.

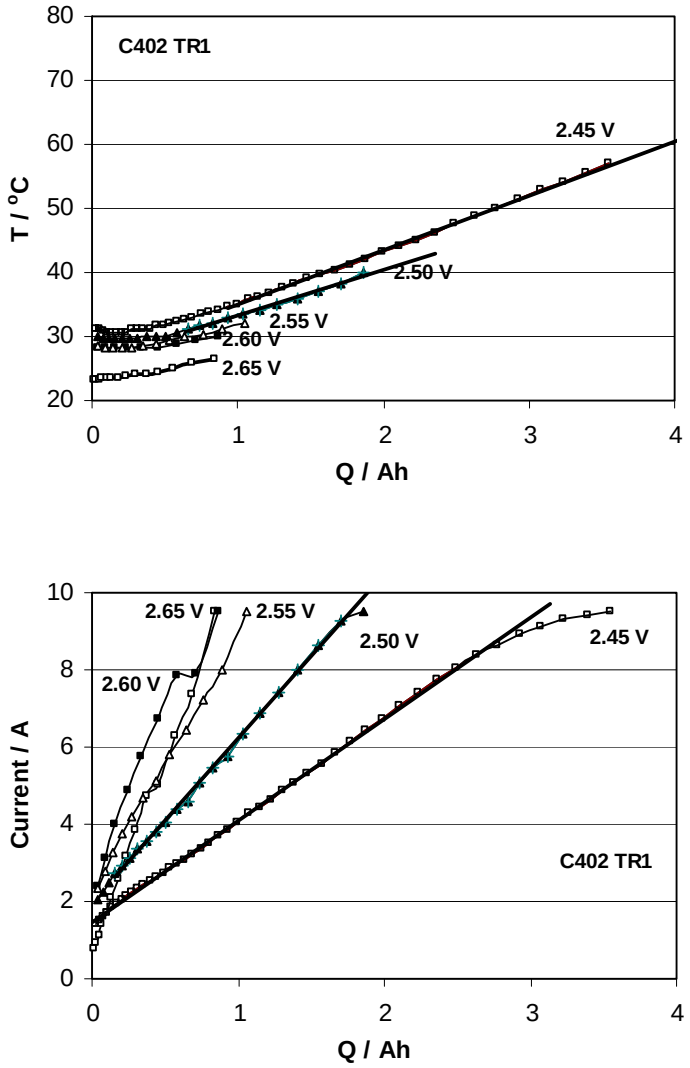

Fig. 5. Dependence of the cell temperature and overcharge current on the electricity accumulated in the cell on different constant voltage overcharges from 2.45 to 2.65 V.

Table 1: Parameters of the equation: $y = a + b*x$ for the cell current and temperature at different polarization voltages

U, V	b(T)	a(T)	b(I)	a(I)
2.45	8.5	26.3	2.6	1.45
2.5	7	26.3	4.3	1.96
2.55	5.1	26.7	6.7	2.26
2.65	5	22.2	10.1	0.7

It can be seen form the data in Fig. 5 and Table 1 that the slope of the linear equation for cell temperature *b* decreases with increase of the cell voltage *U*. The constant *a* in the same equation depends but slightly on the cell polarization voltage. The slope of the linear section in the i/Q curves increases with increase of the applied voltage.

Figure 6 shows the temperature *vs.* current dependence on cell polarization at different constant voltages.

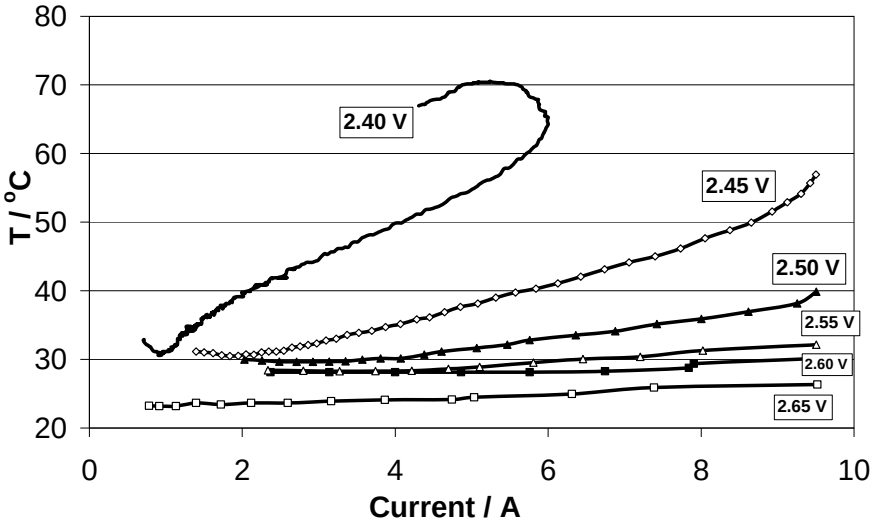

Fig. 6. Dependence of cell temperature on current flowing through the cell during polarization at 2.65 V, 2.60 V, 2.55 V, 2.50 V, 2.45 V and 2.40 V.

To prevent the cell from destruction as a result of the SAIR-TRA effect, the current was limited to maximum 9.5 A. This limited the current increase and the I/Q maximums were not reached at voltages higher than 2.45 V. However, it can be assumed beyond doubt that with increase of *U* the maximum current and temperature values, I_{max} and T_{max}, will be reached if there is no upper current limit.

Within the same range of current values (from 2 to 9.5 A), the cell temperature increases with decrease in cell voltage. This finding is related to the quantity of electricity that flows through the cell as well as with changes in the structures of the interfaces of the two electrodes with the separator. Probably, the latter influence the rates of the chemical reactions that proceed at the two interfaces.

In order to establish the effect of cell polarization voltage and quantity of electricity on the structure of the active masses and of the separators, we performed two series of polarization tests varying the polarization voltage between 2.65 V and 2.40 V at 50 mV steps. Between the two series of tests, the cell was subjected to 10 charge-discharge cycles. Some of the results of the first series of tests were presented in the previous figures. Figure 7a juxtaposes the cell temperature and current dependencies on the quantity of electricity for the two series of tests as well as for the third polarization run at 2.65 V after completion of the second series of tests. The aim of these tests was to determine the conditions for the appearance of the current maximum in the SAIR current transients and of the T_{max} in the TRA temperature curves.

During the first series of polarization tests (TR1) with current limited to I < 9.5 A, the maximum in the i/Q curve appears after 10 Ah of electricity have passed through the cell (i.e. after 6.5 h of polarization) at 2.40 V and I_{max} = 6.0 A, T_{max} = 70^{o}C. During the second series of polarization tests (TR2), the maximum in the current curve appears after 2.5 Ah of electricity have passed through the cell (i.e. 30 min of polarization) at 2.50 V and I_{max} = 8.8 A, T_{max} = 82^{o}C. And finally, a current peak (Imax = 6.6 A) appears at Q_{I} = 2.50 Ah during the third polarization run at 2.65 V and a second peak (I_{max} = 8.0 A) appears at Q_{II} = 12.5 Ah, T_{max} = 96^{o}C. The above results indicate that the SAIR-TRA phenomenon starts after definite structures of the positive and negative active masses, of the separator and of the interface active mass/separator are formed in the cell. An interesting finding is that these structures change for each of the above series of tests tending to impede the SAIR-TRA phenomena and the latter occur at higher cell polarization voltages but after introduction of smaller quantity of electricity into the cell. This finding implies that it is possible to develop a technology for suppressing the SAIR-TRA phenomena within acceptable limits or even for eliminating them. Thus, the harmful thermal effects in valve-regulated lead-acid batteries will be avoided.

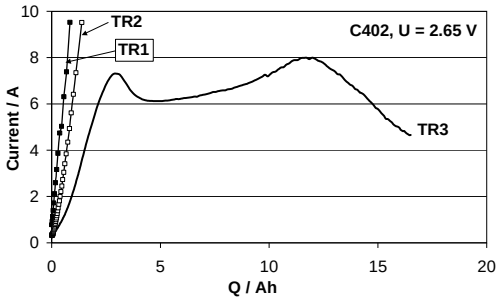
C402, U = 2.65 V
TR2
TR1
TR3
Current / A
Q / Ah

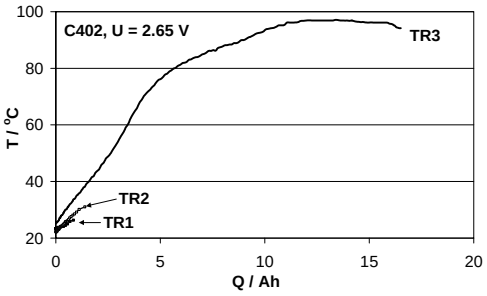
C402, U = 2.65 V
TR3
TR2
TR1
T / °C
Q / Ah

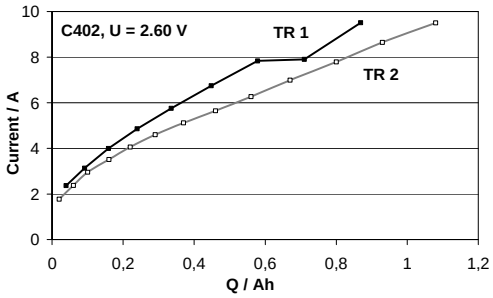
C402, U = 2.60 V
TR 1
TR 2
Current / A
Q / Ah

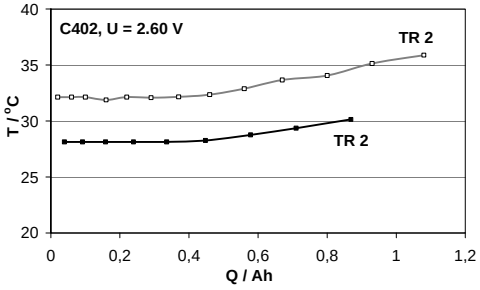
C402, U = 2.60 V
TR 2
TR 2
T / °C
Q / Ah

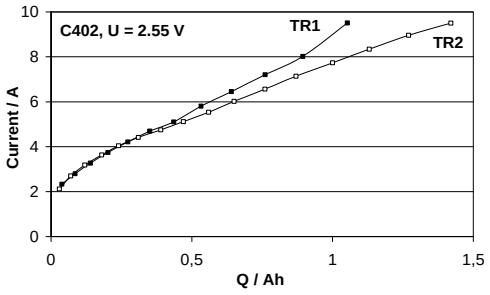
C402, U = 2.55 V
TR1
TR2
Current / A
Q / Ah

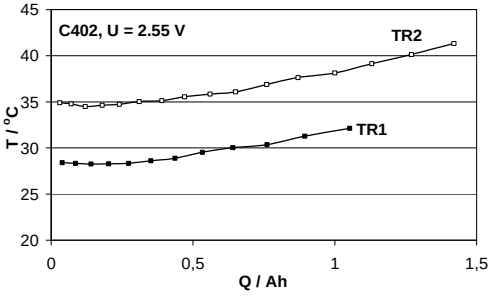
C402, U = 2.55 V
TR2
TR1
T / °C
Q / Ah

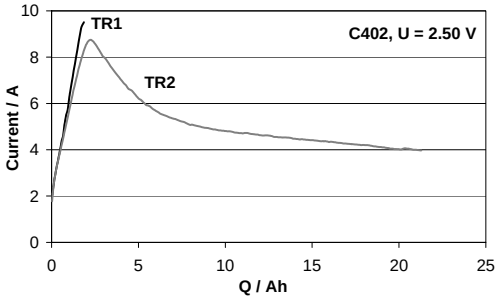
C402, U = 2.50 V
TR1
TR2
Current / A
Q / Ah

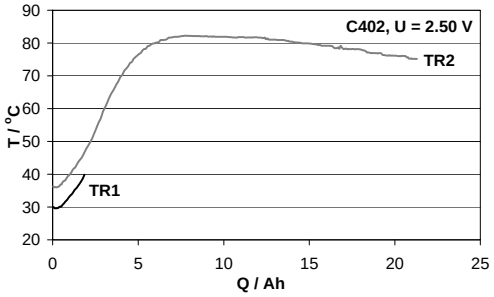
C402, U = 2.50 V
TR2
TR1
T / °C
Q / Ah

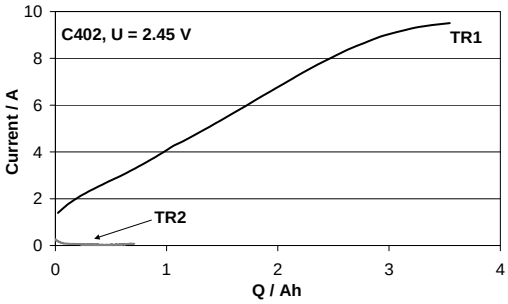
C402, U = 2.45 V
TR1
TR2
Current / A
Q / Ah

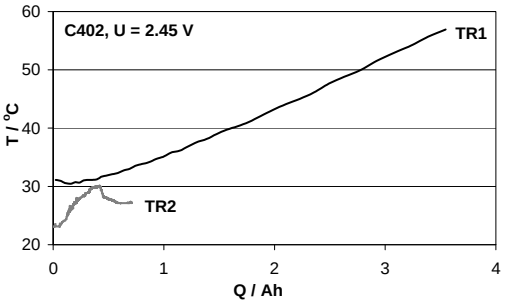
C402, U = 2.45 V
TR1
TR2
T / °C
Q / Ah

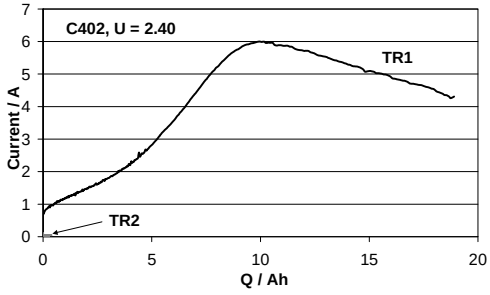
C402, U = 2.40
TR1
TR2
Current / A
Q / Ah

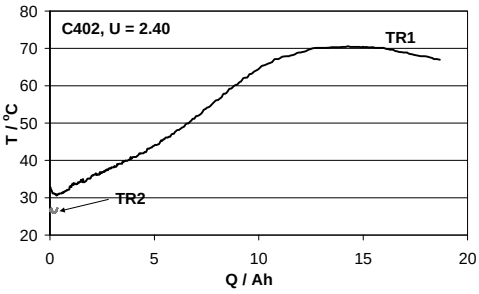
C402, U = 2.40
TR1
TR2
T / °C
Q / Ah

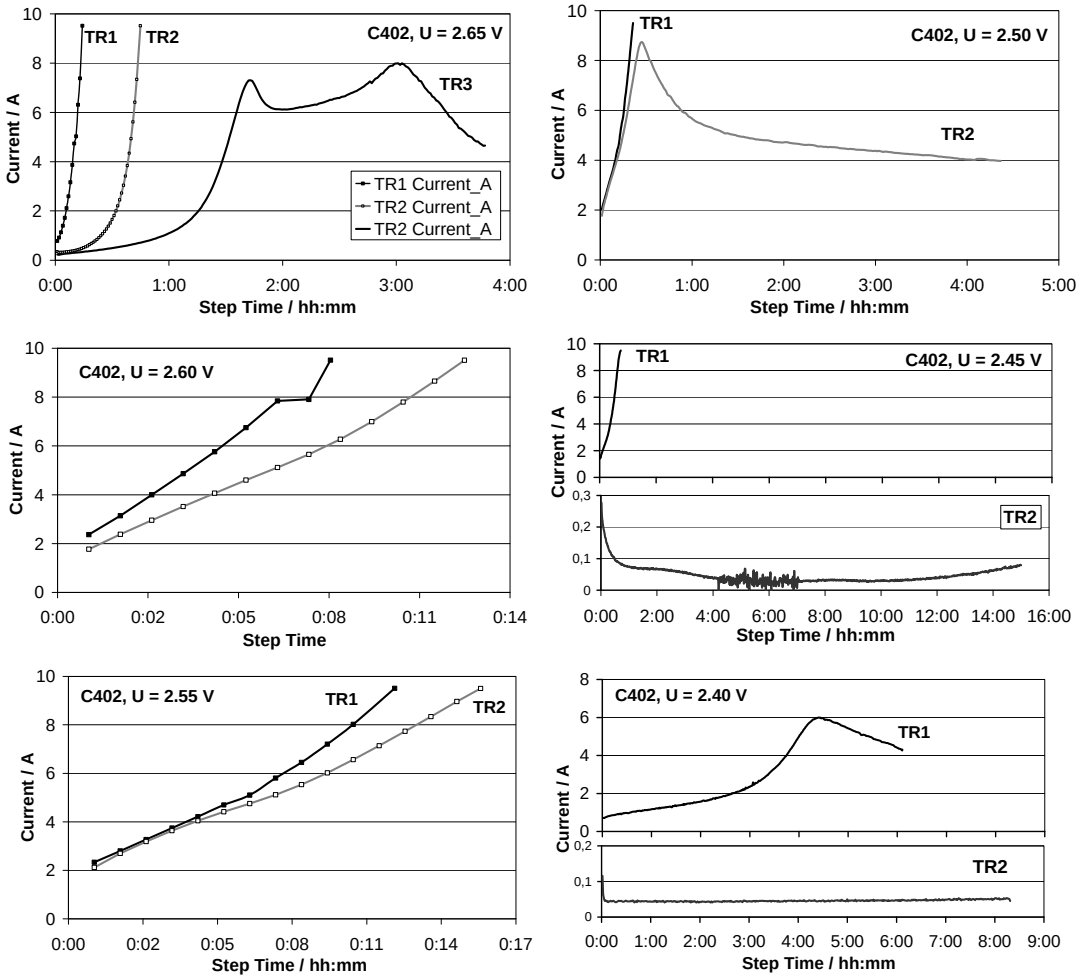

Fig. 7. Cell temperature and overcharge current as a function of the electricity accumulated in the cell at different constant voltage overcharges; (b) Overcharge current *vs*. polarization time at different constant voltage overcharges. ***TR1***, ***TR2*** and ***TR3*** denote three consecutive test series.

The data in Fig. 7 evidence another interesting finding, too, namely that during the second series of polarization tests (TR2) at 2.50 V both I_{max} and T_{max} appear after the first 4-5 Ah of electricity have passed through the cell. During the next polarization run at 2.45 V of the same test series, the current declines instead of increasing and between the 4th and 7th h of polarization the current curve features some oscillations and begins to increase thereafter (TR2 i/t curve, U = 2.45V). On cell polarization at 2.40 V during the TR2 test series the current remains at the 50 mA level for 8.5 hours. This abrupt change in cell behaviour occurs after the SAIR-TRA phenomena have taken place in the cell at 2.50 V and a current of 2 to 8 A has passed through the cell. A 50 mV decrease in polarization voltage causes the cell current to decrease by an order of magnitude. This experimental finding indicates that the SAIR-TRA phenomena have changed the structural components of the cell in such a way that they have lead to qualitative changes in the electrical and thermal behaviour of the cell. It would be interesting to find out what is the nature of these structural changes.

2. Thermal phenomena in MAGM cells

The MAGM cell differs from the AGM one by its high ohmic resistance due to the MAGM separator used. Figure 8 presents the transients for the 5 measured parameters on cell polarization at 2.65 and 2.60 V.

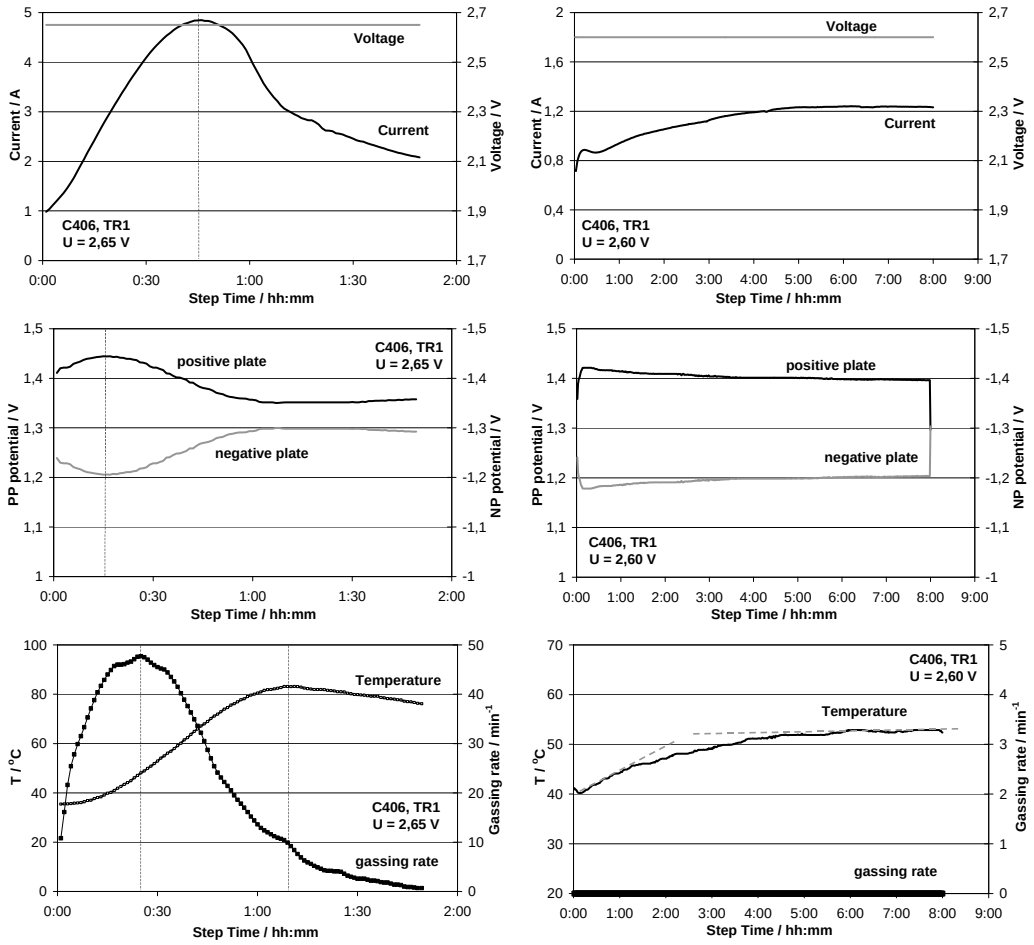

Fig. 8. Changes in U, I, φ^+, φ^-, T^o and gassing rate during cell polarization at constant voltages 2.65 and 2.60 V for the first experimental series.

The processes involved in the SAIR-TRA phenomenon start at the very beginning of cell polarization at 2.65 V and the current peak I_{max} = 6.0A appears after 45 min of polariztaion while $T_{max} = 70^oC$ appears after 1 h and 15 min of polarization.

When the cell is polarized at 2.60 V, a negligible peak I_{max} = 250 mA appears, after which both the current and the temperature increase slowly to reach saturation at i = 1.2 A and $T = 53^oC$. At the above cell polarization voltage no gas evolution from the cell is observed, i.e. the efficiency of the OxCy is 100%. During the steady-state polarization stage, the potential of the positive plate is +1.4 V and that of the negative

plate is –1.2 V, i.e. high enough to keep the electrodes fully charged. Further cell polarization within this test series was continued at 2.40 V at 50 mV steps.

The MAGM cell, too, was subjected to a second series of polarization tests at different voltages. Figure 9 presents the obtained results for cell polarization at 2.65 and 2.60 V, respectively.

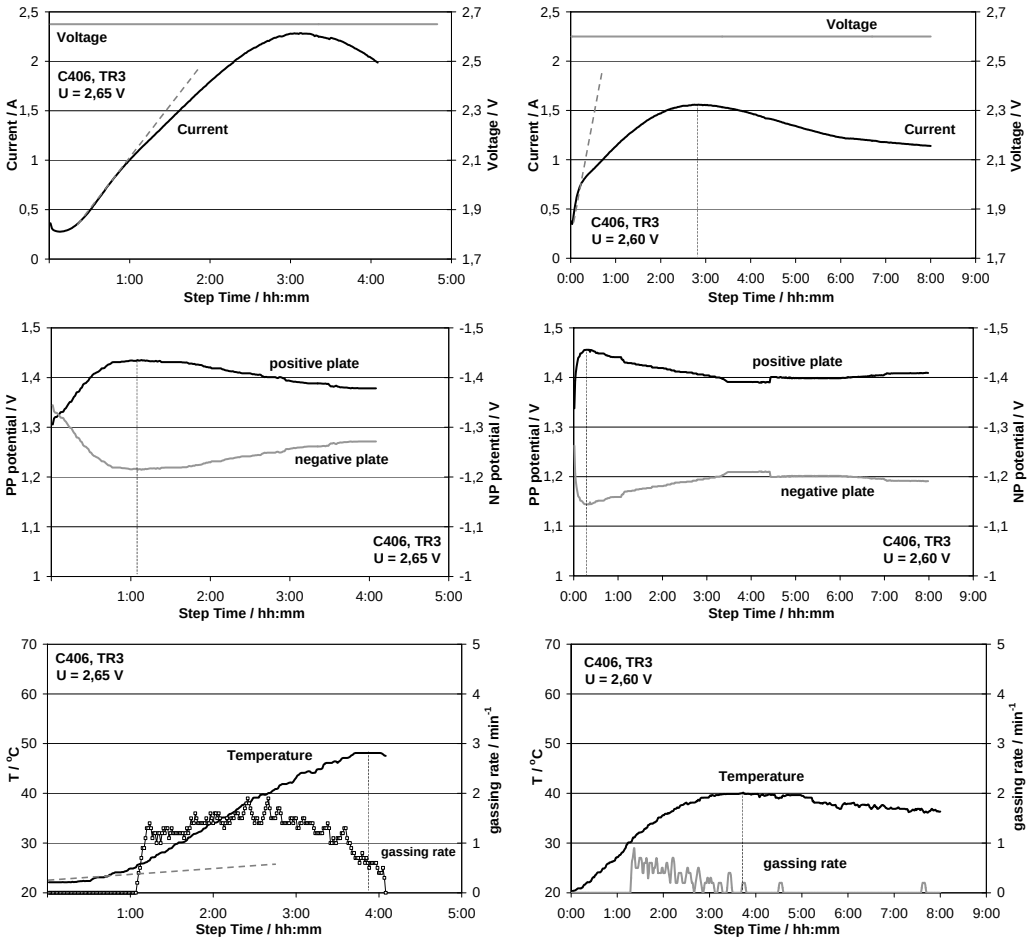

Fig. 9. Changes in U, I, φ^+, φ^-, T^o and gassing rate during cell polarization at constant voltages 2.65 and 2.60 V for the ***TR3*** experimental series.

At both polarization voltages the current and temperature maximums have much lower values. This indicates that the SAIR-TRA phenomenon is strongly suppressed. It does occur but it in a very weak form and till not exert harmful effect on the performance of the cell, because both I_{max} and T_{max} are within the range of values ensuring normal battery operation.

The data in Fig. 7 evidence that in the AGM cell the I_{max} peak appears at 8 A only during the third polarization run at U = 2.65 V and the temperature reaches 98^{o}C, i.e.

a value beyond the range of normal battery operation. Both the AGM and the MAGM cells are assembled with the same types of plates. The only difference between the two cells is the type of separator used. It can be concluded then, that through appropriate selection of the separator for VRLA cells the SAIR-TRA phenomenon can be suppressed to such levels that the cell temperature would not exceed the zone of normal battery operation.

Figure 10 juxtaposes the dependencies of the current *vs.* time of polarization and *vs*. quantity of electricity flowing through the cell as well as the T/Q dependencies for the two series of polarization tests. It can be seen from the data in the figure that the I_{max} peak has shifted towards higher Q values during the second series of polarization tests and the peak is lower and flatter. The rapid increase in current (di/dt) results in higher I_{max} and T_{max} peaks. The i/Q curves at 2.65 V evidence that both (dI/dt) and I_{max} depend on the pre-history of the cell. The SAIR-TRA phenomenon changes the structure in the cell in such a way that both (di/dt) and I_{max} are lower during the subsequent polarization run at the same voltage. This inference is illustrated indirectly by the voltage decrease observed in Fig. 8. Below 2.55 V polarization voltage, no signs of the SAIR-TRA effect are evident. At the same time the oxygen cycle current declines abruptly. This implies that the SAIR-TRA phenomenon creates a memory through the structural changes that occur in the cell.

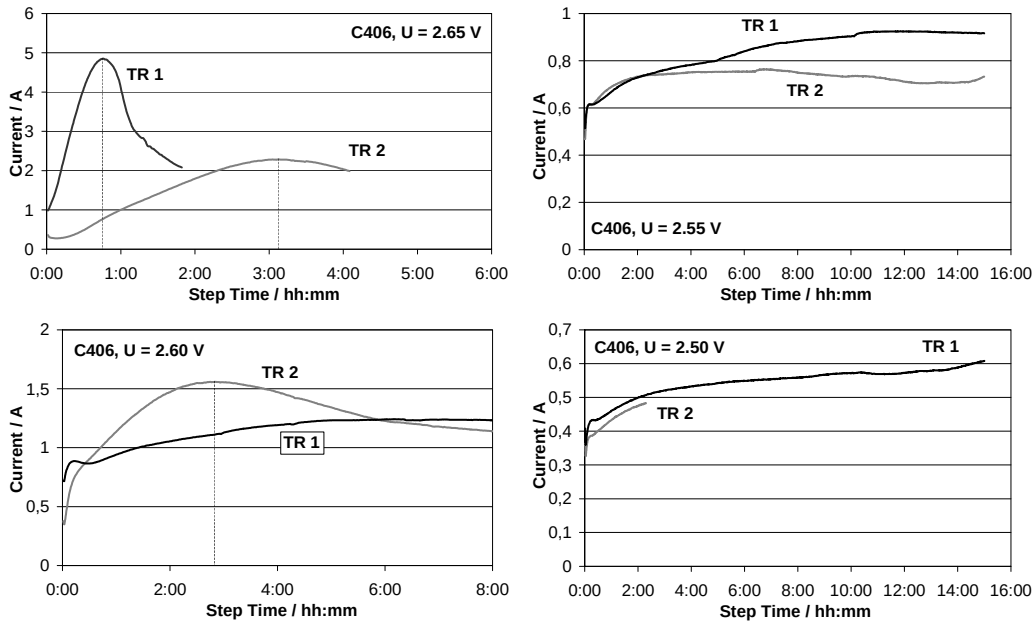

Fig. 10a. Dependence of the overcharge current on time at different constant voltage overcharges: at 2.65 and 2.60 V.

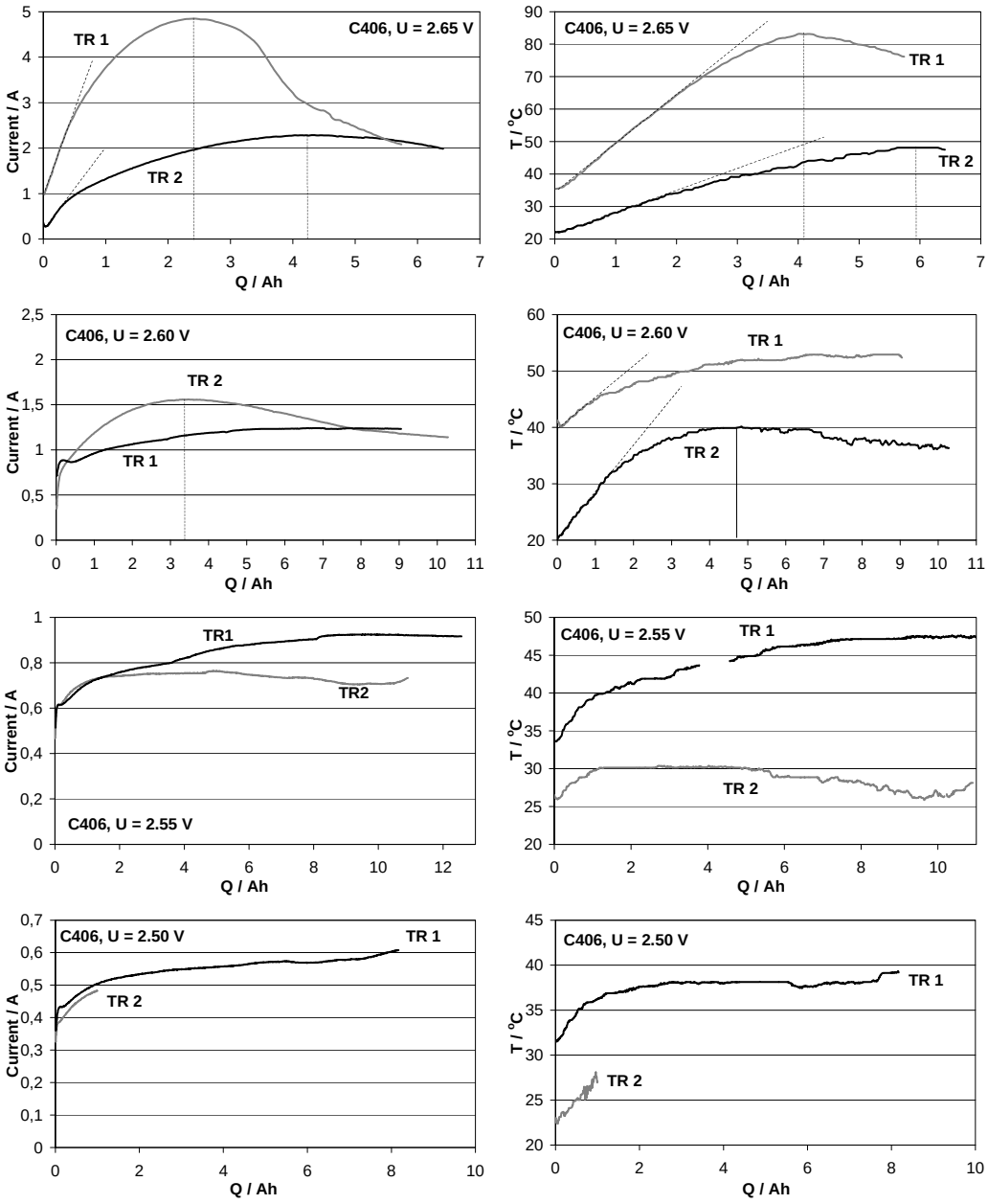

Fig. 10b. Dependence of cell temperature and overcharge current on the electricity accumulated in the cell at different constant voltage overcharges: at 2.65 and 2.60 V. ***TR1*** and ***TR3*** denote two consecutive experimental series.

3. Temperature dependence of cell voltage and of positive and negative plate potentials

These determinations were performed through linear current sweep with a scan rate of 0.1 mA/s at different temperatures: 20°, 30°, 40° and 50°C. The obtained polarization curves for the voltage and the potentials of the positive and negative electrodes of the AGM cell are presented in Fig. 11 for current change from 0 to 1 A, i.e. durign the initial stage of polarization.

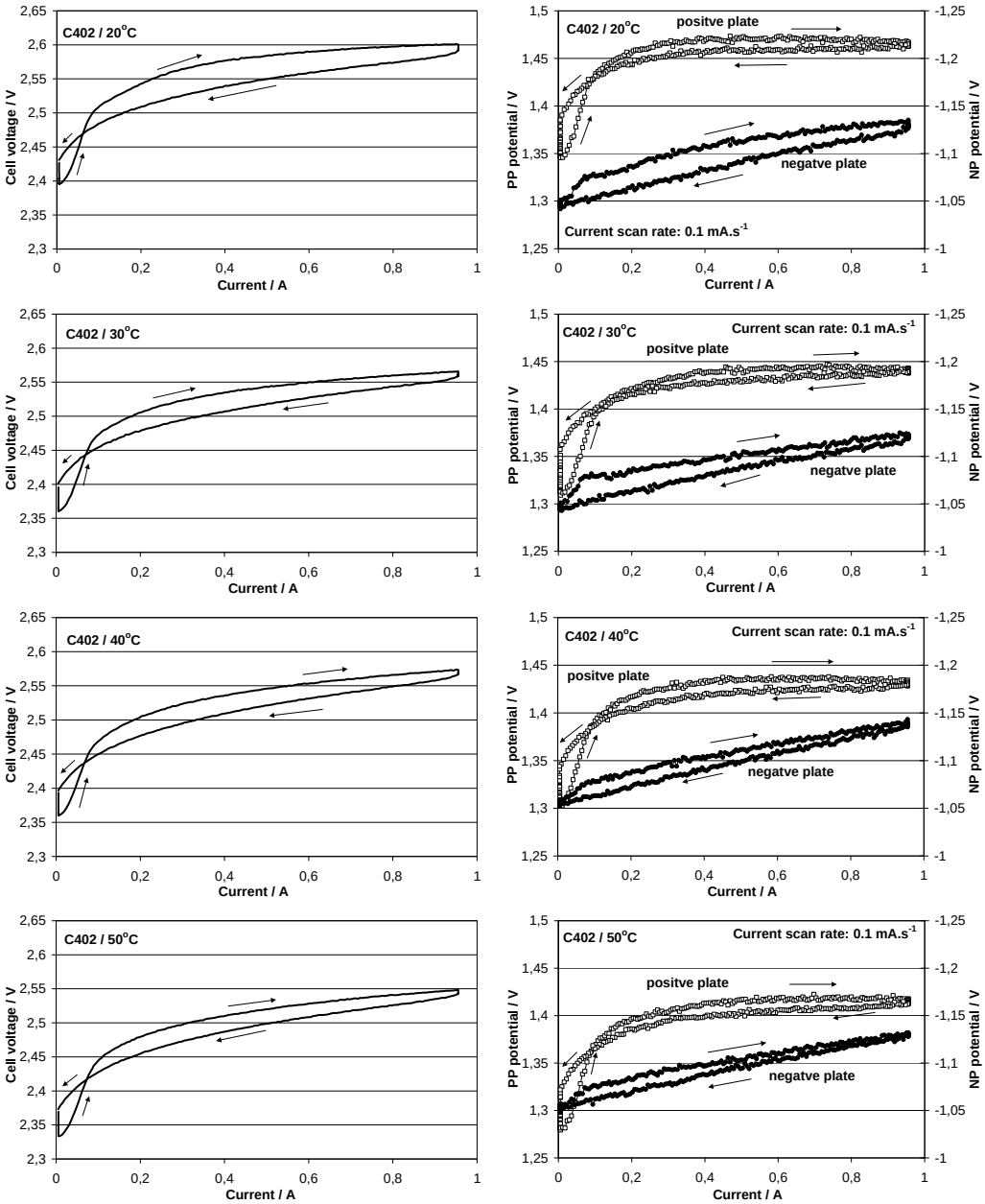

Fig. 11. Changes in potential of the positive and negative plates and in cell voltage with linear sweep current changes at 0.1 mA/min and constant temperatures.

Both electrode curves feature a hysteresis between the anodic and cathodic sweeps. This hysteresis is an indication of some changes in the structure of the interfaces of the two electrodes with the separators. It is at these interfaces that the electrochemical and chemical processes take place. These structural changes during the initial polarization stage affect further progress of the processes.

At the positive electrode, where the decomposition of H_2O to O_2 proceeds, the potential increases abruptly to 0.4 A, after which it depends very slightly or is almost independent of the current. This means that the rate of the reaction of oxygen evolution during the last polarization stage is determined by some chemical or physical elementary process(es) which do not depend on the potential but rather on cell temperature.

The potential of the negative plate depends linearly on the current in both directions of the current sweep. This finding indicates that an electrochemical process is involved in the reduction of oxygen at the negative plate.

The polarization curves for the AGM cell are a sum of polarization curves for the two electrodes. As during the initial polarization stage the potential curve for the positive plate changes more substantially with current changes, its profile will exert a stronger influence on the profile of the cell voltage curve.

The polarization curves for the cell voltage and electrode potentials for the MAGM cell are analogous to those for the AGM cell.

Figure 12 presents the dependencies of the positive and negative plate potentials on cell temperature for the AGM and MAGM cells. The temperature coefficient of the reactions that proceed at the positive plate is 1.7 mV/^{o}C for the AGM cell against 3.3 mV/^{o}C for the MAGM cell. What is this difference due to? It indicates that the interface positive plate/separator influences the temperature coefficient of the positive plate potential, i.e. the process of oxygen evolution.

The temperature exerts almost no influence on the electrochemical processes that take place at the negative plates in the AGM cell. In the MAGM cell the temperature coefficient is 0.7 mV/^{o}C, i.e. the processes at the negative plates are but very slightly affected by the temperature. How can this fact be explained?

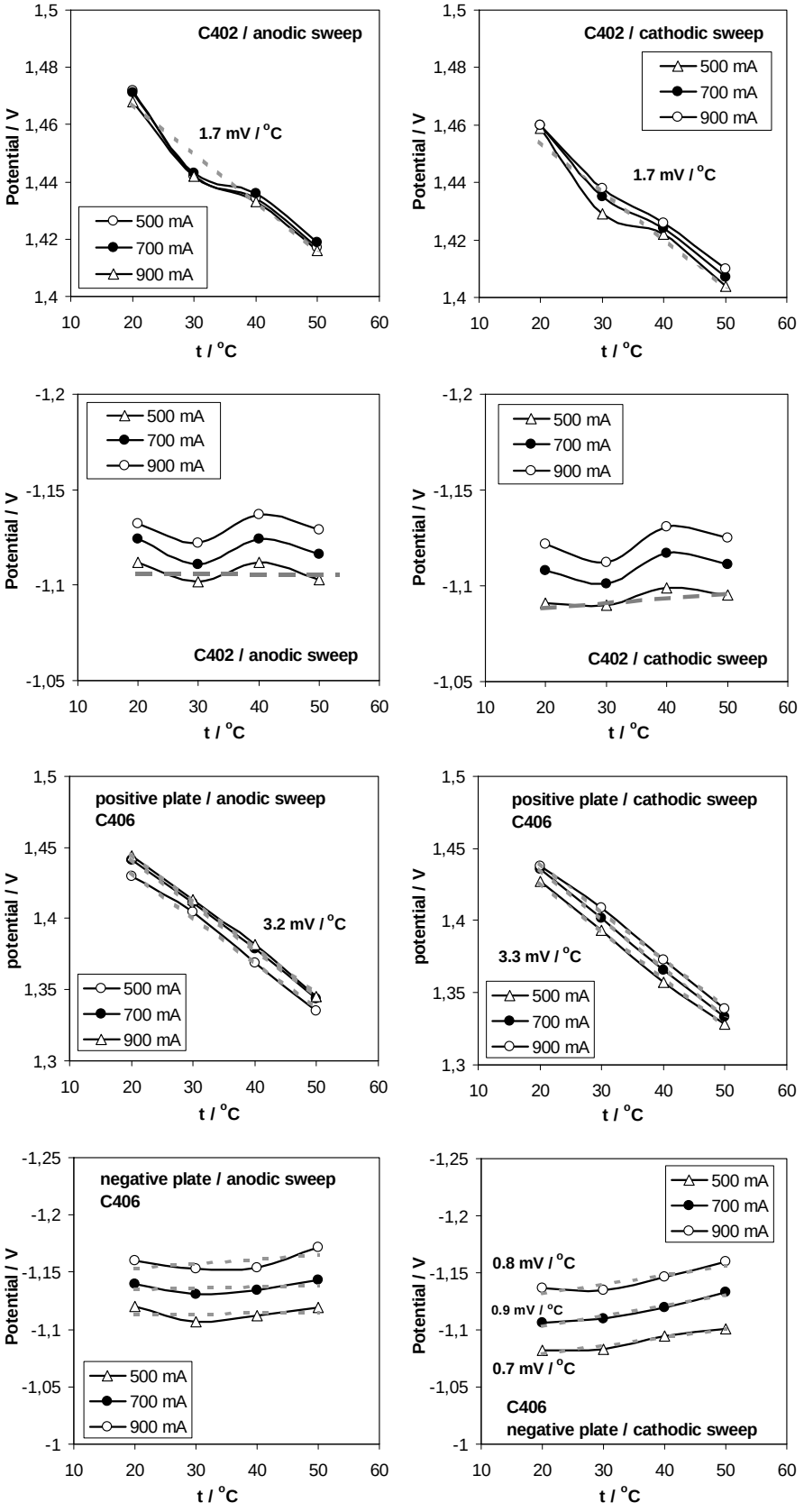

Fig. 12. Potentials of the positive and negative plates as a function of temperature at 3 different currents for AGM (C402) and MAGM (C406) cells. All potentials are measured *versus* an Ag/Ag_2SO_4 reference electrode.

The rate limiting stages in the reaction of oxygen reduction at the negative plate are the diffusion of O_2 through the thin liquid film (TLF) covering the lead surface and the electron transfer [5]. On temperature rise, the amount of O_2 dissolved in the TLF decreases, i.e. the reagent's concentration decreases. On the other hand, the rate of oxygen diffusion through the TLF increases at elevated temperatures. Thus, the two temperature effects compensate each other and hence the potential of the negative plates will be independent of (AGM cell) or will depend but slightly (MAGM cell) on the temperature in the cell.

Figure 12 evidences that at constant cell temperature the current flowing through the negative plate, i.e. the rates of the reactions of oxygen reduction and of hydrogen evolution, depend on the plate potential. In order to increase the current, the potential of the negative plate should be increased. This means that the rates of the above processes at the negative plate depend on some electrochemical elementary process(es).

Generally said, the data in Fig. 12 indicate that the nature and structure of the separator used in VRLA cells exert an influence on the processes that take place at the interfaces of the two types of plates with the separators, the separator influence being very strong on the processes at the interface positive plate/separator. The influence of the separator on the processes at the negative plate is weaker.

4. Analyses of the active materials after the polarization tests

4.1. Active block

AGM cell. The concentration of H_2SO_4 in the AGM separator pores is 1.33 g/cm^3. Severe electrolyte deficiency is observed throughout the whole separator volume. The positive and negative plates are in good condition.

MAGM cell. The H_2SO_4 concentration in the MAGM separator pores is 1.30 g/cm^3. The positive active mass is a bit soft. The active mass in the upper part of the negative plate is lighter in colour than the lower part of the plate.

4.2. Phase composition of the active masses

AGM cell. The XRD patterns for PAM and NAM samples taken from the upepr and lower parts of the plates are presented in Fig. 13.

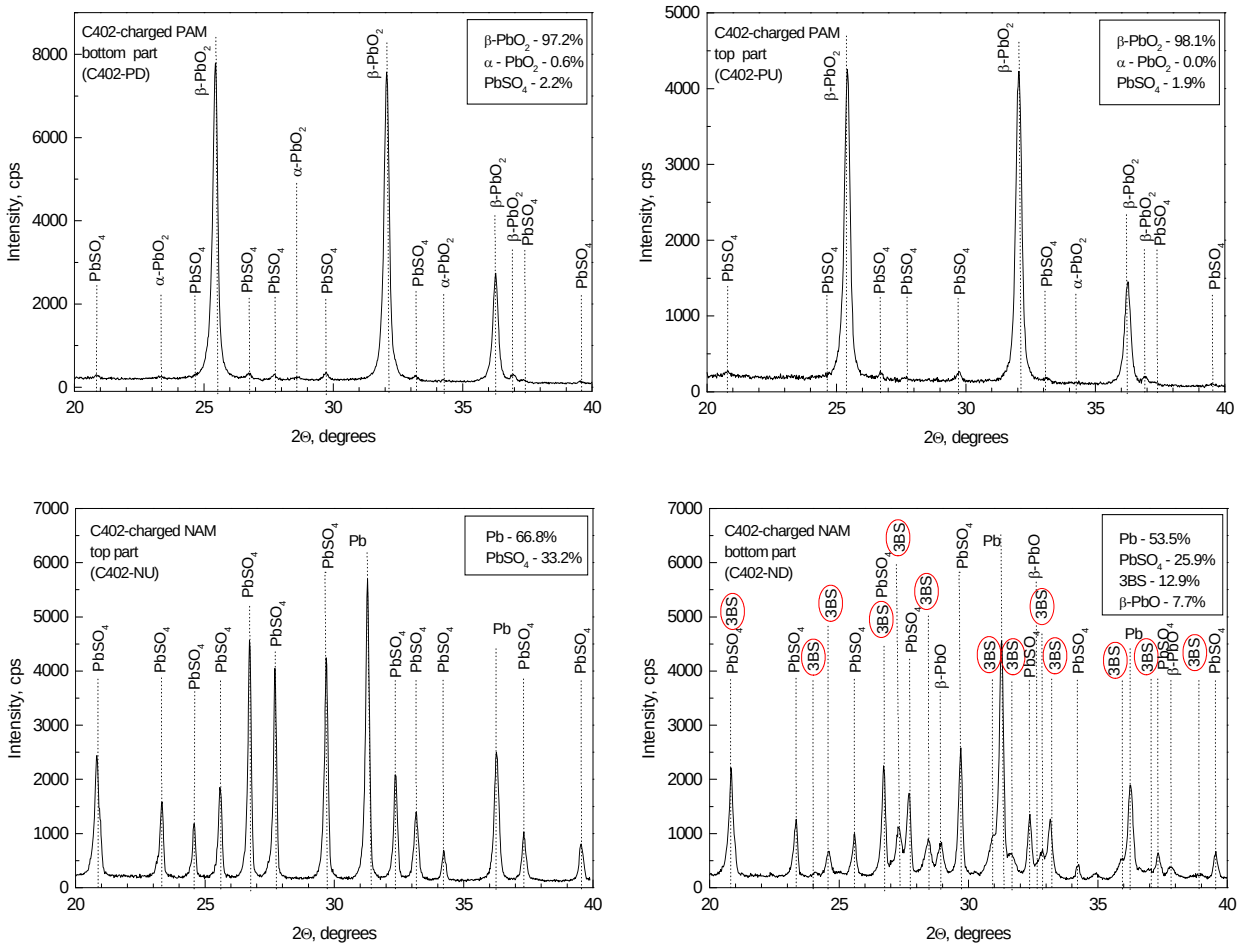

Fig. 13. XRD patterns for PAM samples from the upper and lower parts of the positive and negative plates of the AGM cell.

The positive active mass is composed of βPbO_2 with negligible amounts of $PbSO_4$ and αPbO_2, too. The content of $PbSO_4$ and of αPbO_2 in the lower part of the cell is higher than in the upper part. As has been established in an earlier study of ours [6] at H_2SO_4 concentrations above 1.28 g/cm^3, considerable amounts of αPbO_2 and $PbSO_4$ crystals form, and the acid concentration in the separator of the investigated cell is 1.33 g/cm^3.

The negative active mass comprises Pb and about 33% of $PbSO_4$ in the upper part of the plate, whereas in the lower part the content of $PbSO_4$ is about 26% and 3BS (ca. 13%) and βPbO_2 (ca. 77%) are also detected.

MAGM cell. Figure 14 presents the XRD patterns for PAM and NAM samples taken from the upper and lower parts of the positive and negative plates, respectively.

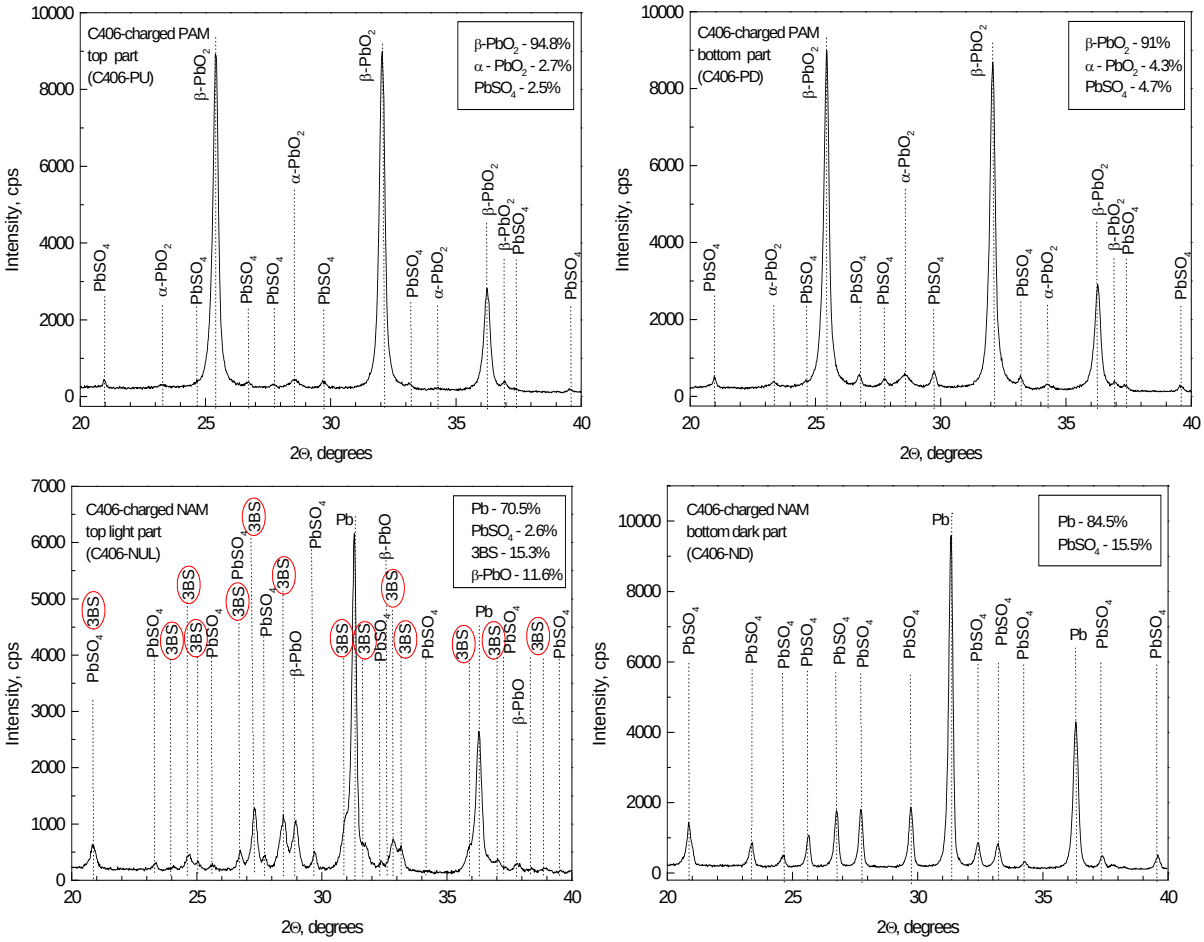

Fig. 14. XRD patterns for PAM samples from the upper and lower parts of the positive and negative plates of the MAGM cell.

The positive active mass contains small amounts of $PbSO_4$ and βPbO_2. With this cell again the content of $PbSO_4$ and βPbO_2 in the lower part of the plate is higher than in the upper part. In the MAGM cell, too, a great part of the Pb is oxidized to $PbSO_4$ throughout the negative plate volume. In the upper part of the negative plate, considerable amounts of 3BS and βPbO are formed. That is the reason for the lower $PbSO_4$ content in the upper part of the plate. The above data represent the phase composition of a peripheral negative plate. The active mass of a central negative plate contains no βPbO and 3BS phases and the content of $PbSO_4$ is between 8 and 16%.

4.3. Structure of the active masses

Figure 15 shows SEM pictures featuring the structure of the lead active mass in the MAGM cell. $PbSO_4$ crystals are clearly seen over the crystals of the lead skeleton

(Fig. 15b,c). Figure 15d features well pronounced 3BS particles. The presence the latter two phases in the active mass is also confirmed by the XRD analyses of NAM.

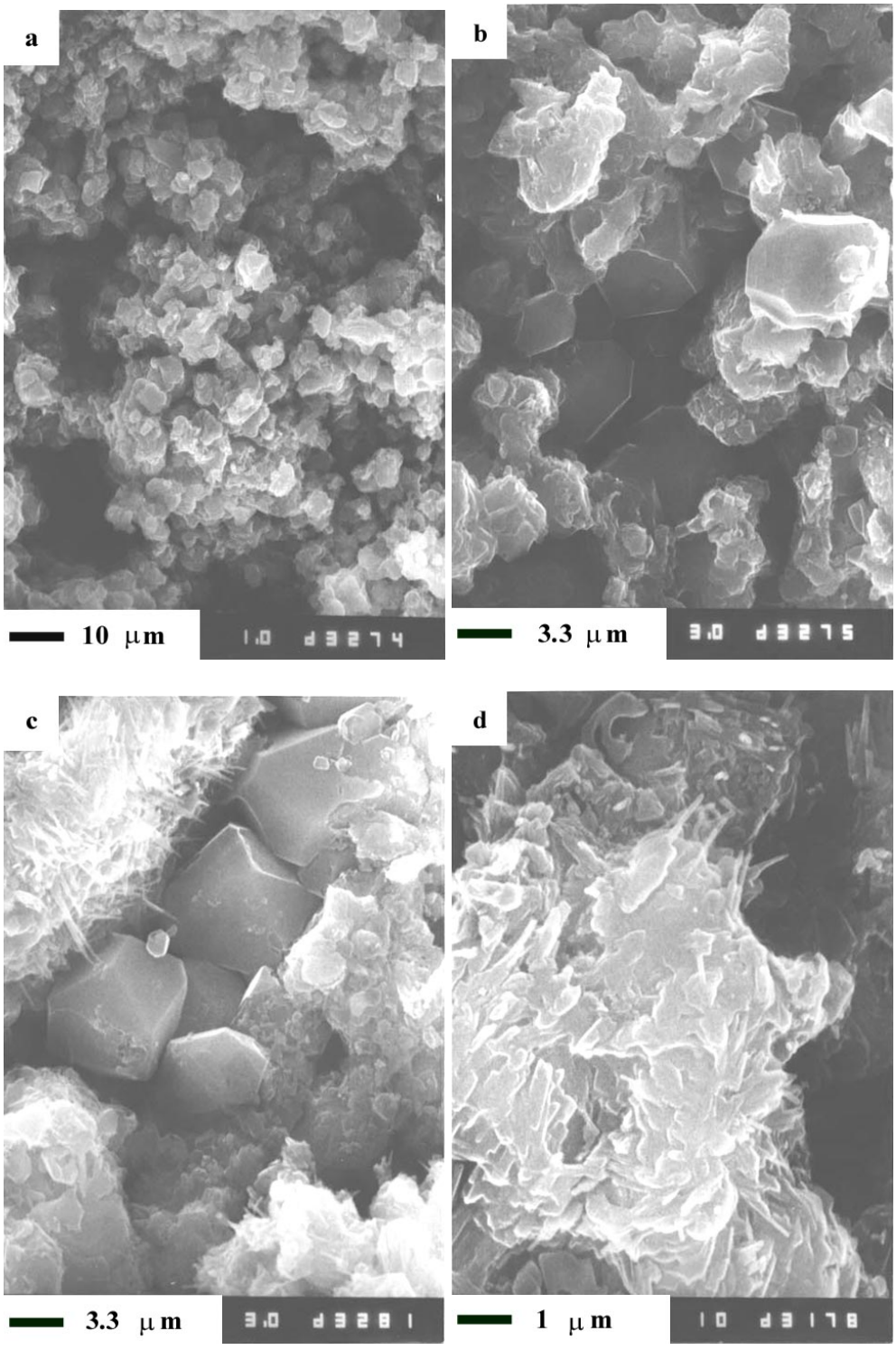

Fig. 15. SEM micrographs of negative active mass sample from MAGM cell.

Figure 16 presents SEM micrographs of the structure of the positive active mass of the MAGM cell.

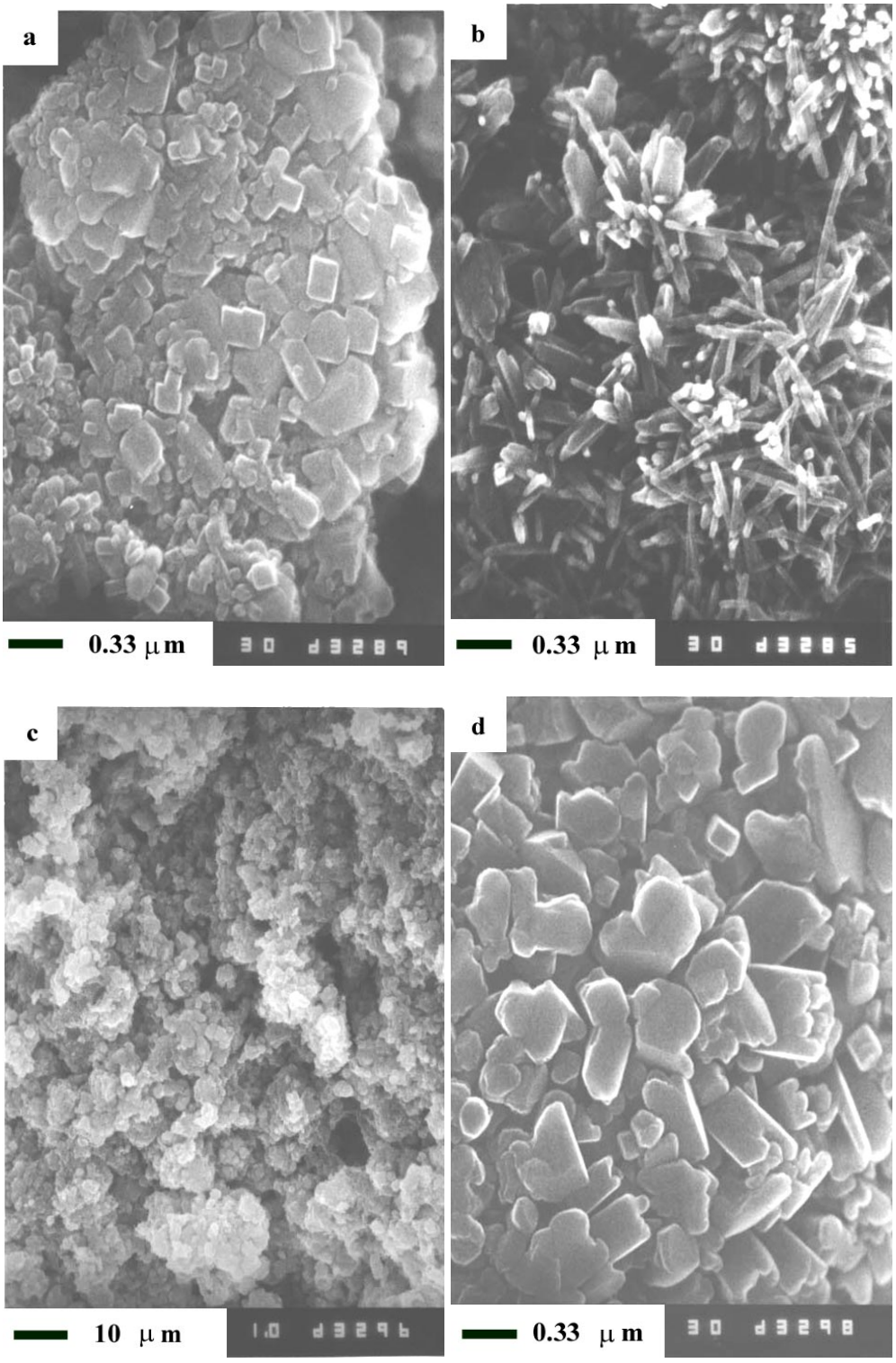

Fig. 16. SEM micrographs of positive active mass sample from MAGM cell.

The PbO_2 particles have crystal (Fig. 16a,d), dendrite (Fig. 16c) or oval (Fig. 16d) shapes. As a rule, crystal βPbO_2 particles are formed in H_2SO_4 solutions with densities higher than 1.29 g/cm^3 [6]. Particles with oval shapes are formed when considerable part of their volume is hydrated. In the latter case the hydrated (gel) zones are responsible for the oval shape of the particles. The positive and negative active masses in the AGM cell have similar structure and crystal morphology as those in the MAGM cell.

5. Chemical and electrochemical reactions involved in the oxygen cycle and proceeding at the two types of electrodes

The following conclusions can be drawn from the above reported experimental results:

(a) The reduction of O_2 at the surface of the negative plate involves an electrochemical reaction. The rate of oxygen reduction depends on the potential of the plate (Figs. 11 and 12).

(b) The reduction of O_2 at the lead surface of the negative plate involves chemical reactions. This is manifested by the fact that the temperature rises whereas the current (i.e. the rate of the electrochemical reaction) decreases (Figs. 3, 6 and 10) as well as by the presence of $PbSO_4$, 3BS and PbO phases in the negative active mass (Figs. 13 and 14).

(c) The chemical reactions that proceed in the cell release heat as a result of which the temperature in the cell rises. Figure 6 evidences that the temperature rises despite the decrease in current.

(d) Hydrogen is evolved at the negative plate, which indicates that the efficiency of oxygen reduction is not always 100% (Fig. 2: 2.50 V, 2.45 V and 2.40 V; Fig. 8: TR1 – 2.65 V, TR2 – 2.65 V and 2.60 V). It has been established that hydrogen may be involved in the process of oxygen reduction [7].

Let us now see what reactions can proceed at the two electrodes:

At the positive plate, an electrochemical reaction of water decomposition and evolution of oxygen proceeds.

$$2H_2O \rightarrow O_2 + 4H^+ + 4e^- \qquad (1)$$

The gradual consumption of water increases the concentration of H_2SO_4 at the interface positive plate/separator. The pressure of the evolved oxygen in the interface

layer increases and an oxygen flow moves through the separator to the negative plate. Another oxygen flow leaves the active block thus increasing the gas pressure above this block. When this pressure exceeds a definite value, the cell vent opens and the gas leaves the cell.

At the negative plate, oxygen may be reduced through several mechanisms, which are discussed below. All these mechanisms result in the formation of water. Consequently, the H_2SO_4 concentration in the lead active mass pores decreases.

5.1. Electrochemical mechanism of oxygen reduction with no involvement of the lead surface

According to this mechanism the following reaction proceeds:

$$O_2 + 2H^+ + 2e^- \leftrightarrows H_2O_2 \qquad (2)$$

This reaction is known to be a fast one and to proceed when oxygen is reduced on Hg substrate [8], Ag-Au [9,10], Ag-Cu-Hg [11], Au [12], Pt and platinated Pt [13], Hg [14] and Ni [15]. There is no reason to assume that Pb will be an exception. The formation of H_2O_2 on oxygen reduction has been established through the reduction of O_2 enriched with ^{18}O isotope [16]. The same percent contents of ^{18}O-^{18}O and ^{18}O-^{16}O have been found in H_2O_2 as in the initial (primary) oxygen. Hence, the conclusion has been drawn that the O-O bond in the oxygen molecule does not break during reduction of O_2 to H_2O_2.

H_2O_2 is in a strongly reducing medium in lead surface/TLF layer. So it may be further reduced by the following mechanisms:

(a) electrochemical mechanism

$$H_2O_2 + 2H^+ + 2e^- \rightarrow 2H_2O_2 \qquad (3)$$

This is a slow reaction and proceeds at considerable overvoltages. This reaction has been investigated for Hg [8,17,18], Pt [113,19] and gold [12] substrates. It has been established that the reduction involves non-dissociated H_2O_2 molecules.

However, beside through reaction (3), H2O2 may be reduced also through the following chemical reactions and at a high rate at that. All these reactions release

heat which accelerates further the rates of the chemical reactions. The following substances serve as reducers:

(b) reduction with hydrogen participation [5] – parallel to reaction (2) a reaction of hydrogen evolution proceeds at the lead surface:

$$2H^+ + 2e^- \rightarrow 2H \qquad (4)$$

Part of the evolved hydrogen (θ) forms molecules and leaves the cell together with an equivalent amount of oxygen that has not reacted by reaction (2). The rate of this gas flow is measured with the help of a flowmeter.

$$2\theta H \rightarrow \theta H_2 \qquad (5)$$

Another part of the evolved hydrogen (1-θ) reacts with H_2O_2 through the following chemical reaction:

$$2(1-\theta)\ H + (1-\theta)\ H_2O_2 \rightarrow 2(1-\theta)\ H_2O \qquad (6)$$

Hydrogen atoms are a strong reducer and H_2O_2 is a strong oxidizer. Both products are formed simultaneously at the lead surface and react with each other as a result of which heat is released. The ratio between the rates of reactions (5) and (6) determine the efficiency of the oxygen cycle. If the rate of reaction (6) is much higher than that of reaction (5), the efficiency of the oxygen cycle is high and *vice versa*.

(c) reaction between H_2O_2 and Pb

H_2O_2 oxidizes the lead surface throught he following chemical reaction:

$$H_2O_2 + Pb \rightarrow PbO + H_2O \qquad (7)$$

Heat is released by this reaction. PbO may be reduced to Pb through the electrochemical reaction

$$PbO + 2H^+ + 2e^- \rightarrow Pb + H_2O \qquad (8)$$

whereby water is formed and the lead surface is rebuilt. In the above case the Pb surface plays a catalytic role by accelerating the reduction of H_2O_2.

However, PbO may also react with H_2SO_4 forming $PbSO_4$ and releasing heat.

$$PbO + H_2SO_4 \rightarrow PbSO_4 + H_2O \qquad (9)$$

$PbSO_4$ is reduced to Pb through the electrochemical reaction of charge:

$$PbSO_4 + 2H^+ + 2e^- \rightarrow Pb + H_2SO_4 \quad (10)$$

Reactions (8) and (9) are in competition. Reaction (10) may proceed at a low rate and though the plate is discharged, certain amounts of $PbSO_4$, PbO and basic lead sulfates may form in the negative active mass as a result of reactions (7) and (9). These are indeed detected by the XRD analyses (Figs. 13 and 14).

5.2. Chemical mechanism of oxygen reduction through oxidation of the lead surface

The oxygen oxidizes the lead surface, whereby heat is released:

$$O_2 + 2Pb \rightarrow 2PbO \quad (11)$$

Then PbO may be reduced through the electrochemical reaction (8) or be sulphated (reaction (9)) and the obtained $PbSO_4$ may then be reduced through reaction (10).

Figures 11 and 12 evidence that the reduction of O_2 at the negative plate proceeds through an electrochemical reaction (e.g. reaction 2). Then the obtained H_2O_2 is involved in various chemical and electrochemical reactions. So if reaction (11) does proceed, it has but a very small share in the overall process of oxygen reduction.

All chemical reactions involved in the above described mechanisms are associated with heat release. Depending on the conditions at the interface plate/separator, the various reactions will compete with each other. Thus for example reactions (2) and (11), reactions (8) and (9), etc. As a result of this competition, different amounts of heat will be released and hence the SAIR-TRA effect will manifest itself to different extents and the OxCy will have different efficiency. The occurrence of reactions in which Pb is involved is also demonstrated by the considerable amounts of $PbSO_4$, 3BS and PbO phases detected in the negative active mass. The retarded reduction of the above compounds leads to discharge of the negative plate. On the other hand, the reduced efficiency of the oxygen cycle results in water loss and in partial discharge of the negative plate. This is often observed with stationary batteries.

On the other hand, the creation of conditions facilitating the chemical reactions leads to the SAIR-TRA effect. The flow of strong current through the cell, when the SAIR process take place, generates more Joule heat, which added to the heat effects of the above reactions, contributes further to the generation of heat in the cell.

CONCLUSIONS

1. Appropriate equipment has been designed and constructed for monitoring 6 parameters of the lead-acid cell during operation of the oxygen cycle.
2. It has been established that thermal problems occur in the battery on constant voltage overcharge above a definite voltage. Under the above conditions, after a certain quantity of electricity has passed through the cell, the processes at the positive and at the negative plates get into a self-accelerating interrelation. As a result of this interrelation the current increases reaching a maximum value i_{max} within a certain period of time. Parallel to the increase in current, the cell temperature rises, too, until a maximum value T_{max}. The i_{max} and T_{max} peaks appear after different quantities of electricity flow through the cell and they represent “the two sides of a coin”, i.e. the two sides of one and the same phenomenon: SAIR (*self-accelerating interrelation between the reactions of the OxCy)* reflects the current increase and TRA (*thermal runwaway*) – the temperature rise. So we could designate the overall phenomenon as SAIR-TRA.
3. The mechanism of the SAIR-TRA phenomenon has been disclosed. Four stages of this phenomenon have been distinguished and the processes involved in each of these stages have been identified and the interrelation between these processes has been studied.
4. It has been established that the intensity of the SAIR-TRA phenomenon depends on the voltage applied to the cell, the type of separator used and the pre-history of the cell before the occurrence of the phenomenon. Through appropriate selection of the above parameters during the cell design process, it is possible to slow down or suppress the SAIR-TRA phenomenon to such an extent as to prevent the current and temperature from rising beyond the range of values ensuring normal battery operation.
5. The temperature coefficients of the potentials of the positive and negative plates have been determined under conditions of operative oxygen cycle. The temperature coefficient of the positive plate potential is found to be between 1.7 and 3.5 $mV/^oC$, whereas that of the negative plate potential is very small or equal to zero. This latter value is attributed to the influence of temperature on the dissolution of oxygen in the H_2SO_4 solution covering the lead surface of the negative plate and to its diffusion through the thin liquid film covering the lead surface.

6. It has been established that at lower efficiencies of the oxygen cycle, some process may take place at the negative plates that may limit the capacity of these plates and hence the battery capacity will decline. This effect of the OxCy on the performance of the battery can be avoided through selection of appropriate mode of battery operation as well as through some technological improvements.

General conclusion: All planned activities within the Work Program of the present Project have been completed successfully and the end goal of the project has been achieved.

What should be done within a next stage of investigations of the SAIR-TRA phenomenon?

The basic mechanism of the processes causing the SAIR-TRA effect has been disclosed within the present project. Future research efforts should be focused in two directions:

I. Oxygen cycle

To find methods to control the SAIR-TRA phenomenon. To achieve this aim it is necessary:

(a) to perform thermodynamic investigations of the OxCy processes and to identify the reactions with the smallest thermal effect;
(b) to find separators that can suppress the SAIR-TRA phenomenon within normal battery operation limits.

II. Lead-acid batteries

To establish the influence of the OxCy processes on the performance characteristics of the battery through:

(a) determining the changes caused by the SAIR-TRA phenomenon on battery performance (mainly on capacity);
(b) finding battery design solutions to reduce (suppress) the SAIR-TRA effect on battery performance.

Our laboratory, the Lead-Acid Batteries Department of the Institute of Electrochemistry and Energy Systems (former CLEPS), has all necessary equipment, hardware and software, as well as highly qualified and experienced research personnel, capable of achieving the above goals within a period of 2-3 years. If the US Army European Research Office is interested, we are ready to negotiate on the scope, term and cost of a second stage of the TRA Project.

The present report will be submitted for publication in the *Journal of Power Sources* after minor revision.

Literature cited

1. Project title “Mechanism of thermal runaway in VRLA batteries and methods to suppress it”, 1st Interim Report, Jan. 2004.

2. Project title “Mechanism of thermal runaway in VRLA batteries and methods to suppress it”, 2nd Interim Report, May 2004.

3. Project title “Mechanism of thermal runaway in VRLA batteries and methods to suppress it”, 3rd Interim Report, Oct. 2004.

4. D. Pavlov, *J. Power Sources*, **64** (1997) 131.

5. A. Kirchev, D. Pavlov, B. Monahov, *J. Power Sources*, **113** (2003) 245.

6. D. Pavlov, A. Kirchev, M. Stoycheva, B. Monahov, *J. Power Sources*, **137** (2004) 288.

7. D. Pavlov, A. Kirchev, B. Monahov, *J. Power Sources*, (in press).

8. J. Heyrowsky, *Cas. cesk. Lekarn.*, **7** (1927) 242.

9. A.I. Krasilshtikov, *J. Phys. Chem.* (rus), **21** (1947) 849.

10. A.I. Krasilshtikov, *J. Phys. Chem.* (rus), **23** (1949) 332.

11. G. Siver, B.N. Kabanov, *J. Phys. Chem.* (rus), **22** (1948) 53.

12. I.M. Kolthoff, J. Jordan, *J. Am. Chem. Soc.*, **47** (1952) 4801.

13. S. Winkelmann, *Z. Elektrochem*., **60** (1956) 731.

14. M.V. Stackelberg, Polarographische Arbeitsmethoden, Berlin, 1950, s. 172.

15. A.I. Krasilshtikov, B.A. Abdreeva, *J. Phys. Chem.* (rus), **27** (1953) 389.

16. M.C. Davies, M. Clark, E. Yeger, F. Hovorka, *J. Electrochem. Soc.*, **106** (1959) 56.

17. J.O’M. Bockris, L.F. Oldfild, *Trans. Faraday Soc*., **51** (1955) 248.

18. A.I. Krasilshtikov, *J. Phys. Chem.* (rus), **26** (1952) 216.

19. R. Gerischer, H. Gerischer, *Z. phys. Chem*. (N.F.), **6** (1956) 178.

Annex 1

ARL–ERO RESEARCH PROJECT STATEMENT

Project title: ***"MECHANISM OF THERMAL RUNAWAY IN VRLA BATTERIES AND METHODS TO SUPPRESS IT"***

CONTRACT NUMBER: **N62558-03-M-0805**

Contractor Name: **Central Laboratory of Electrochemical Power Sources (CLEPS) Lead-Acid Batteries Dept.**

Address: **Acad. G. Bonchev street, block 10, Sofia 1113, Bulgaria**
Phone: +359 2 718651 Fax: +359 2 731552

Total amount funded: **$50,000.00 for 12 months**

Expenditures to date: **$50,000.00 for Interim Reports No.1, No. 2, No. 3 and Final Report**

Unused funds remaining: **$0.00**

Principal Investigator: **Prof. DETCHKO PAVLOV**

Address: Central Laboratory of Electrochemical Power Sources (CLEPS)
Lead-Acid Batteries Dept.
Acad.G. Bonchev street, block 10, Sofia 1113, Bulgaria

Signature: …….. Date: 10.12.2004